EPJ manuscript No.
(will be inserted by the editor)

Possible Molecular States Composed of Doubly Charmed Baryons with Couple-channel Effect

Bin Yang[1a], Lu Meng[1b], and Shi-Lin Zhu[1,2,3c]

[1] School of Physics and State Key Laboratory of Nuclear Physics and Technology, Peking University, Beijing 100871, China
[2] Center of High Energy Physics, Peking University, Beijing 100871, China
[3] Collaborative Innovation Center of Quantum Matter, Beijing 100871, China

arXiv:1906.04956v1 [hep-ph] 12 Jun 2019

Received: date / Revised version: date

Abstract. We systematically investigate the possible molecular states composed of (1) two spin-$\frac{3}{2}$ doubly charmed baryons, and (2) a pair of spin-$\frac{3}{2}$ and spin-$\frac{1}{2}$ doubly charmed baryons. The one-boson-exchange (OBE) model is used to describe the potential between two baryons. The channel mixing effect is considered for the systems with the same quantum number ($I(J^P)$) but different total spin (S) and orbital angular momenta (L). We also study the channel mixing effect among the systems composed of various doubly charmed baryons if they have the same quantum number. Many of the systems are good candidates of molecular states.

PACS. XX.XX.XX No PACS code given

1 Introduction

The researches on exotic states attract much attention since the first charmonium-like exotic state $X(3872)$ was reported by the Belle Collaboration [1] in 2003. After that, more and more exotic states have been observed by many major experimental collaborations, such as CLEO-c, BaBar, Belle, BESIII, CDF, D0, LHCb and CMS. Those states include charmonium-like states such as $Z_c(3900)$ [2, 3,4], $Y(4260)$ [5,6], $Y(4140)$ [7], and bottomonium-like states, $Z_b(10610)$ and $Z_b(10650)$ [8] and so on. In 2015, the LHCb Collaboration discovered two pentaquark states $P_c(4380)$ and $P_c(4450)$ in the J/Ψ invariant mass spectrum of the $\Lambda_b^0 \to J/\Psi K^- p$ decay [9]. Recently, the LHCb Collaboration reported that $P_c(4450)$ was resolved into two states $P_c(4440)$ and $P_c(4457)$ and observed a lower state $P_c(4312)$ [10]. The experimental and theoretical progress about exotic states can be found in the recent reviews [11, 12,13,14,15,16,17,18].

Some multiquark exotic states are near the threshold of two hadrons. They might be molecular states. A hadronic molecular state is a loosely bound system composed of two color-singlet hadrons. The two hadrons are bound together by the residual force of the color interaction. One can use the One-boson-exchange (OBE) model to describe the dynamics between the two baryons in a molecular system. The OBE model is very successful to describe the deuteron as a hadronic molecular state composed of a neutron and a proton. The meson exchange force together with the couple-channel effect between S-wave and D-wave renders the deuteron a loosely bound state.

About forty years ago, Voloshin and Okun proposed the hadronic molecule composed of two heavy mesons [19]. De Rujula *et al.* interpreted the $\psi(4040)$ as a $D^*\bar{D}^*$ molecule in Ref. [20]. Törnqvist used the one-pion-exchange (OPE) potential to calculate the possible charmed meson-antimeson molecular state [21,22]. Besides, there are also many other calculations about possible hadronic molecular states, such as the combination of two mesons [23,24,25,26,27,28,29], or two baryons [30,31,32,33,34,35,36]. Similarly, one can also explain the hidden charm pentaquark states as a molecular state formed by one heavy meson and one heavy baryon [37,38,39,40,41,42,43,44,45].

In 2017, the LHCb collaboration reported the doubly charmed baryon Ξ_{cc} at $3621.40 \pm 0.72(\text{stat}) \pm 0.27(\text{syst}) \pm 0.14(\Lambda_c^+)$ MeV in the $\Lambda_c^+ K^- \pi^+ \pi^+$ mass spectrum [46]. As an important member in the baryon family, there are many theoretical works to calculate the mass of the doubly charmed baryon [47,48,49,50,51,52,53,54]. It is also very interesting to investigate the possible molecular states containing doubly charmed baryons. The system composed of Ξ_{cc} and a charmed meson or baryon was calculated in Refs. [55,56]. The possible molecular system with Ξ_{cc} and a nucleon is studied in Refs. [57,35].

In Ref. [34], the authors investigated the possible deuteron-like bound states composed of two spin-$\frac{1}{2}$ doubly charmed baryons in the SU(3) flavor symmetry. In this work, we extend the same formalism to investigate the possible hadronic

[a] e-mail: bin_yang@pku.edu.cn
[b] e-mail: lmeng@pku.edu.cn
[c] e-mail: zhusl@pku.edu.cn

molecular states composed of two spin-$\frac{3}{2}$ doubly charmed baryons (include Ξ_{cc} and Ω_{cc}), denoted as B^*B^*, as well as system one spin-$\frac{3}{2}$ and one spin-$\frac{1}{2}$ baryon, denoted as B^*B. We use the OBE model to describe the potential between two baryons. The couple-channel effect among B^*B^*, B^*B and two spin-$\frac{1}{2}$ baryons, BB, are also included in this work. When we calculate the pure B^*B^* and B^*B systems, we consider the couple-channel effect from D-wave and G-wave.

We organize this work as follows. We give the theoretical formalism in Section 2, including the effective Lagrangian, coupling constants and the effective interaction potentials. We present the numerical results of the B^*B^* systems and the B^*B systems in Section 3. In the calculation, we also include the couple-channel effect among BB, B^*B and B^*B^*. Then we discuss our results and conclude in Section 4. In Appendixes A and B, we collect some useful formulae and functions. We also calculate the systems composed of one baryon and one antibaryon, such as $B^*\bar{B}^*$ and $B^*\bar{B}$. The results are collected in Appendix C.

2 Formalism

For a doubly charmed baryon, the two charm quarks can be treated as a static color source in the heavy quark limit. For the two charm quarks, their color wave function should be in the antisymmetric $\bar{3}_c$-representation. The spatial wave function of the two charm quarks is symmetric for the ground state. As a consequence, their spin wave function must be symmetric because of the Pauli principle. Therefore, the total spin of the two charm quark is 1, and the total spin of a ground doubly charmed baryon is $\frac{1}{2}$ or $\frac{3}{2}$. In the present work, we focus on the possible deuteron-like systems composed of two doubly charmed baryons with both spin-$\frac{3}{2}$, or one spin-$\frac{3}{2}$ baryon and one spin-$\frac{1}{2}$ baryon. The systems with the same quantum number but different components may couple with each other. We include the couple-channel effect in this work.

2.1 The Lagrangian

For convenience, we use column matrices to describe the doubly charmed baryons as follows,

$$B=\left[\Xi_{cc}^{+}\ \Xi_{cc}^{++}\ \Omega_{cc}^{+}\right]^{T},\quad B^{*\mu}=\left[\Xi_{cc}^{*+}\ \Xi_{cc}^{*++}\ \Omega_{cc}^{*+}\right]^{\mu T}, \tag{1}$$

where B and $B^{*\mu}$ denote the spin-$\frac{1}{2}$ and spin-$\frac{3}{2}$ baryons, respectively. The exchanged mesons between two baryons are denoted by two matrices as follows,

$$\mathcal{M}=\begin{bmatrix}\frac{\pi^0}{\sqrt{2}}+\frac{\eta}{\sqrt{6}} & \pi^+ & K^+\\ \pi^- & -\frac{\pi^0}{\sqrt{2}}+\frac{\eta}{\sqrt{6}} & K^0\\ K^- & \bar{K}^0 & -\frac{2}{\sqrt{6}}\eta\end{bmatrix},$$
$$\mathcal{V}^{\mu}=\begin{bmatrix}\frac{\rho^0}{\sqrt{2}}+\frac{\omega}{\sqrt{2}} & \rho^+ & K^{*+}\\ \rho^- & -\frac{\rho^0}{\sqrt{2}}+\frac{\omega}{\sqrt{2}} & K^{*0}\\ K^{*-} & \bar{K}^{*0} & \phi\end{bmatrix}^{\mu}, \tag{2}$$

where $\mathcal{M}$ and $\mathcal{V}^{\mu}$ denote the octet pseudoscalar mesons and the nonet vector mesons, respectively.

We construct the effective Lagrangian as follows,

$$\mathcal{L}=\mathcal{L}_{\sigma hh}+\mathcal{L}_{phh}+\mathcal{L}_{vhh}, \tag{3}$$

for the scalar meson exchange

$$\mathcal{L}_{\sigma hh}=g_{\sigma BB}\bar{B}\sigma B-g_{\sigma B^*B^*}\bar{B}^{*\mu}\sigma B^*_{\mu}, \tag{4}$$

for the pseudoscalar meson exchange

$$\begin{aligned}\mathcal{L}_{phh}=&-\frac{g_{pBB}}{2m_B}\bar{B}\gamma_\mu\gamma_5\partial^\mu\mathcal{M}B+\frac{g_{pB^*B^*}}{2m_{B^*}}\bar{B}^{*\mu}\gamma_\nu\gamma_5\partial^\nu\mathcal{M}B^*_\mu\\&+\frac{g_{pB^*B}}{m_B+m_{B^*}}\bar{B}^*_\mu\partial^\mu\mathcal{M}B+h.c.,\end{aligned} \tag{5}$$

and for the vector meson exchange

$$\begin{aligned}\mathcal{L}_{vhh}=&g_{vBB}\bar{B}\gamma_\mu\mathcal{V}^\mu B+\frac{f_{vBB}}{2m_B}\bar{B}\sigma_{\mu\nu}\partial^\mu\mathcal{V}^\nu B\\&-g_{vB^*B^*}\bar{B}^{*\mu}\gamma_\nu\mathcal{V}^\nu B^*_\mu\\&-i\frac{f_{vB^*B^*}}{2m_{B^*}}\bar{B}^*_\mu(\partial^\mu\mathcal{V}^\nu-\partial^\nu\mathcal{V}^\mu)B^*_\nu\\&+i\frac{f_{vB^*B}}{2\sqrt{m_{B^*}m_B}}\bar{B}^*_\mu(\partial^\mu\mathcal{V}^\nu-\partial^\nu\mathcal{V}^\mu)\gamma_\nu\gamma_5B+h.c..\end{aligned} \tag{6}$$

The notations $g_{\sigma B^{(*)}B^{(*)}}$, $g_{pB^{(*)}B^{(*)}}$, $g_{vB^{(*)}B^{(*)}}$ and $f_{vB^{(*)}B^{(*)}}$, represent the coupling constants. m_B and m_{B^*} are the masses of the spin-$\frac{1}{2}$ and spin-$\frac{3}{2}$ heavy baryons, respectively.

2.2 Coupling constants

The coupling constants in the effective Lagrangian (4-6) should be extracted from the experiment data. However there are no experiment data for the doubly charmed baryon scattering with light mesons. Thus, we compare the coupling constants of doubly charmed baryons with the ones of the nucleons, which are known. With the help of the quark model, we get the relations between the coupling constants of doubly charmed baryons and nucleons. The details of this method can be found in Ref. [60]. Here we directly show the relations between the two sets of coupling constants,

– scalar meson exchange

$$g_{\sigma BB}=g_{\sigma B^*B^*}=\frac{1}{3}g_{\sigma NN}, \tag{7}$$

Table 1. The relevant hadron masses [46,54,58] and coupling constants for the nucleon [59,60,61,62]. For the multiple hadrons, their averaged masses are used.

Baryons	Mass(MeV)	Mesons	Mass(MeV)	Mesons	Mass(MeV)	Couplings	Value
Ξ_{cc}	3621.4	σ	600	ρ	775.49	$g^2_{\sigma NN}/4\pi$	5.69
Ω_{cc}	3778	π	137.25	ω	782.65	$g^2_{\pi NN}/4\pi$	13.6
Ξ^*_{cc}	3686	η	547.85	ϕ	1019.46	$g^2_{\rho NN}/4\pi$	0.84
Ω^*_{cc}	3872	K	495.65	K^*	893.77	$f_{\rho NN}/g_{\rho NN}$	6.1

– pseudoscalar meson exchange

$$g_{pBB} = -\frac{\sqrt{2}}{5}\frac{m_B}{m_N}g_{\pi NN}, \tag{8}$$

$$g_{pB^*B^*} = \frac{3\sqrt{2}}{5}\frac{m_{\Xi^*_{cc}}}{m_N}g_{\pi NN}, \tag{9}$$

$$g_{pB^*B} = \frac{2\sqrt{6}}{5}\frac{m_B + m_{B^*}}{2m_N}g_{\pi NN}, \tag{10}$$

– vector meson exchange

$$\begin{aligned} g_{vBB} &= \sqrt{2}g_{\rho NN} \\ g_{vBB} + f_{vBB} &= -\frac{\sqrt{2}}{5}(g_{\rho NN} + f_{\rho NN})\frac{m_B}{m_N}, \end{aligned} \tag{11}$$

$$\begin{aligned} g_{vB^*B^*} &= \sqrt{2}g_{\rho NN} \\ g_{vB^*B^*} + f_{vB^*B^*} &= \frac{3\sqrt{2}}{5}(g_{\rho NN} + f_{\rho NN})\frac{m_{B^*}}{m_N}, \end{aligned} \tag{12}$$

$$\begin{aligned} g_{vB^*B} &= 0 \\ f_{vB^*B} &= -\frac{2\sqrt{6}}{5}\frac{\sqrt{m_{B^*}m_B}}{m_N}(g_{\rho NN} + f_{\rho NN}). \end{aligned} \tag{13}$$

In the above formula, $g_{\sigma NN}$, $g_{\pi NN}$ $g_{\rho NN}$ and $f_{\rho NN}$ are the corresponding coupling constants of nucleons. The values of them are taken from Refs. [59,60,61,62]. In this work, we choose three nuclear coupling constants as input. The coupling constant $g_{\pi NN}$ is stable in various models compared with $g_{\omega NN}$ and $g_{\eta NN}$. Therefore, we use the unified parameter of the nucleon-nucleon-π vertex for the pseudoscalar meson exchange. For the vector meson exchange, we choose the parameter of the ρ meson exchange vertex for the same reason. Their values are given in Table 1. We give the values of the coupling constants for doubly charmed baryons in Table 2.

2.3 The effective potentials

We give the effective Lagrangian in Section 2.1. One can write the effective potentials in the momentum space for two doubly charmed baryons with the Lagrangians (4-6). The effective potentials $V(Q)$ is a function of the momentum of the exchanged mesons. In the non-relativistic limit, we reserve the scattering amplitude up to $\mathcal{O}(\frac{1}{m_Q^2})$, where m_Q is the mass of the doubly charmed baryon. Given that the baryons are not fundamental point particles, we introduce a form factor $\mathcal{F}(\boldsymbol{Q})$ at each baryon-baryon-meson vertex,

$$\mathcal{F}(\mathbf{Q}) = \frac{\Lambda^2 - m_{ex}^2}{\Lambda^2 - Q^2} = \frac{\Lambda^2 - m_{ex}^2}{\lambda^2 + \mathbf{Q}^2}, \tag{14}$$

where $\lambda^2 = \Lambda^2 - Q_0^2$. m_{ex} is the mass of the exchanged mesons. The parameter Λ is an adjustable momentum cutoff, which can suppress the contribution of the high momentum transferred. We use the factor to roughly describe the effect of the baryon structure. As a low energy effective model, the OBE potential should not contain very short-range interactions. Therefore, adopting the form factor keeps the model self-consistent. The parameter Λ can not be strictly determined without any experiment data. The value of Λ is around an empirical scale, 1 GeV. The possible binding energy of a two baryon system depends on the parameter, as we shall show in Section 3. Then we transform the effective potential together with the form factor to coordinate space,

$$V(r) = \frac{1}{(2\pi)^3}\int d\boldsymbol{Q}e^{i\boldsymbol{Q}\cdot\boldsymbol{r}}V(\boldsymbol{Q})\mathcal{F}^2(\boldsymbol{Q}). \tag{15}$$

The total effective potential is as follows,

$$V(r) = V^s(r) + V^p(r) + V^v(r). \tag{16}$$

The superscripts s, p and v are used to mark the scalar, pseudoscalar and vector mesons exchange potentials. The potentials can be divided into four terms. They are the central potential term, the spin-spin interaction term, the spin-orbit interaction term and the tensor term. The spin-spin, spin-orbit and tensor terms contain the spin-spin operator Δ_{SS}, spin-orbit operator Δ_{LS} and tensor operator Δ_T, respectively. The specific definition of those angular momentum dependent operators are different for the systems composed of baryons with different spins. We will discuss the operators in detail after we introduce the couple-channel effect. Here we use subscripts C, SS, LS, T to mark them respectively. We derive the general potentials between two doubly charmed baryons in the specific formulae for different mesons exchanged as follows.

Table 2. The coupling constants for the doubly charmed baryons.

	$g_{\sigma BB}$	g_{pBB}	g_{vBB}	f_{vBB}		$g_{\sigma B^*B^*}$	$g_{pB^*B^*}$	$g_{vB^*B^*}$	$f_{vB^*B^*}$		g_{pB^*B}	f_{vB^*B}
$\Xi_{cc}\Xi_{cc}$	2.82	-14.26	4.60	-29.76	$\Xi^*_{cc}\Xi^*_{cc}$	2.82	43.55	4.60	72.25	$\Xi^*_{cc}\Xi_{cc}$	49.84	-87.95
$\Xi_{cc}\Omega_{cc}$	2.82	-14.57	4.60	-30.30	$\Xi^*_{cc}\Omega^*_{cc}$	2.82	44.65	4.60	74.16	$\Xi^*_{cc}\Omega_{cc}$	50.91	-89.83
$\Omega_{cc}\Omega_{cc}$	2.82	-14.88	4.60	-30.85	$\Omega^*_{cc}\Omega^*_{cc}$	2.82	45.75	4.60	76.12	$\Xi_{cc}\Omega^*_{cc}$	51.11	-90.14
										$\Omega^*_{cc}\Omega_{cc}$	52.18	-92.07

– For the scalar meson exchange,

$$\begin{aligned} V^s(r) =& V^s_C(r,\sigma) + V^s_{LS}(r,\sigma), \\ V^s_C(r) =& -C^s_\sigma \frac{g_{\sigma 1} g_{\sigma 2}}{4\pi} u_\sigma \left[H_0 - \frac{u^2_\sigma}{8 m_a m_b} H_1 \right], \\ V^s_{LS}(r) =& -C^s_\sigma \frac{g_{\sigma 1} g_{\sigma 2}}{4\pi} \frac{u^3_\sigma}{2 m_a m_b} H_2 \Delta_{LS}. \end{aligned} \tag{17}$$

– For the pseudoscalar meson exchange,

$$\begin{aligned} V^p(r) =& \sum_{\alpha=\pi,\eta,K} \left[V^p_{SS}(r,\alpha) + V^p_T(r,\alpha) \right], \\ V^p_{SS}(r,\alpha) =& C^p_\alpha \frac{g_{p1} g_{p2}}{4\pi} \frac{u^3_\alpha}{12 m_a m_b} H_1 \Delta_{SS}, \\ V^p_T(r,\alpha) =& C^p_\alpha \frac{g_{p1} g_{p2}}{4\pi} \frac{u^3_\alpha}{12 m_a m_b} H_3 \Delta_T. \end{aligned} \tag{18}$$

if $u^2_\alpha < 0$, the potentials change into

$$\begin{aligned} V^p_{SS}(r,\alpha) =& C^p_\alpha \frac{g_{p1} g_{p2}}{4\pi} \frac{\theta^3_\alpha}{12 m_a m_b} M_1 \Delta_{SS}, \\ V^p_T(r,\alpha) =& C^p_\alpha \frac{g_{p1} g_{p2}}{4\pi} \frac{\theta^3_\alpha}{12 m_a m_b} M_3 \Delta_T, \end{aligned} \tag{19}$$

where $\theta^2_\alpha = -u^2_\alpha$.

– For the vector meson exchange,

$$\begin{aligned} V^v(r) =& \sum_{\beta=\omega,\rho,\phi,K^*} \left[V^v_C(r,\beta) + V^v_{SS}(r,\beta) + V^v_T(r,\beta) + V^v_{LS}(r,\beta) \right], \\ V^v_C(r,\beta) =& C^v_\beta \frac{u_\beta}{4\pi} \left[g_{v1} g_{v2} H_0 + \frac{u^2_\beta}{8 m_a m_b} (g_{v1} g_{v2} + 2 g_{v1} f_{v2} + 2 g_{v2} f_{v1}) H_1 \right], \\ V^v_{SS}(r,\beta) =& C^v_\beta \frac{1}{4\pi} \left[g_{v1} g_{v2} + g_{v1} f_{v2} + g_{V2} f_{v1} + f_{v1} f_{v2} \right] \frac{u^3_\beta}{6 m_a m_b} H_1 \Delta_{SS}, \\ V^v_T(r,\beta) =& -C^v_\beta \frac{1}{4\pi} \left[g_{v1} g_{v2} + g_{v1} f_{v2} + g_{v2} f_{v1} + f_{v1} f_{v2} \right] \frac{u^3_\beta}{12 m_a m_b} H_3 \Delta_T, \\ V^v_{LS}(r,\beta) =& -C^v_\beta \frac{1}{4\pi} \left[3 g_{v1} g_{v2} \Delta_{LS} + 4 g_{v1} f_{v2} \Delta_{LS_a} + 4 g_{v2} f_{v1} \Delta_{LS_b} \right] \frac{u^3_\beta}{2 m_a m_b} H_2. \end{aligned} \tag{20}$$

In the above expressions, $u_{\sigma/\alpha/\beta}$ are defined as $u^2_{ex} = m^2_{ex} - Q^2_0$, where m_{ex} is the mass of the exchanged meson. Q_0 is the zeroth component of the transition momentum. In the heavy baryon limit, Q_0 can be easily expressed with mass differences between the initial and final baryons. For the system composed of two baryons with masses m_1 and m_2, the value of the Q_0 is 0 for the direct diagram. For the cross diagram, the value of the Q_0 is $|m_1 - m_2|$. m_a and m_b are the masses of two doubly charmed baryons. For the initial and the final baryons of one Fermion line with the mass splitting, we approximately choose the geometric means of their masses, $m_a = \sqrt{m_{ai} m_{af}}$. In Table 1 we give the masses of the baryons, as well as the masses of the exchanged mesons. For the multiple hadrons, their averaged masses are used.

g_s, g_p and g_v are the coupling constants in Eqs. (7-13). The subscript 1 and 2 of the coupling constants are used to mark different vertices. C^s_σ, C^p_α and C^v_β are the isospin factors. Their values are given in Table 3. For a system composed of different baryons, we should consider both direct and cross diagrams, as in Fig. 1. In Table 3 we use "[ ]" to denote the isospin factors of the cross diagrams. The functions $H_i = H_i(\Lambda, m_{\sigma/\alpha/\beta}, r)$ and $M_i = M_i(\Lambda, m_\alpha, r)$ come from the Fourier transformation. We give their specific expressions in Appendix A.

For the system composed of one baryon and one antibaryon, the Lagrangians (4-6) still work. For the process exchanging a meson with certain G-parity, I_G, the potentials are the Eqs. (17-20) with the extra G-parity factor I_G. With the help of the G-parity rule, we can directly write

down the effect potentials of the baryon and antibaryon systems. We let the isospin factors of baryon-antibaryon system absorb the extra G-parity factor. The values are also given in Table 3.

For some systems, some terms in the Lagrangian are lacking. Their potentials can be described with part of the formulae (4-6). In those cases we can also directly use the same potential but set the relevant coupling constant to zero.

We consider the couple-channel effect between states with different orbital angular momentum. The spin of a system composed of two spin-$\frac{3}{2}$ baryons can be 0, 1, 2 and 3. For a $J = 0$ system, we consider the couple-channel effect between $^1S_0$ and $^5D_0$. For a $J = 1$ system, we consider four channels, $^3S_1$, $^3D_1$, $^7D_1$ and $^7G_1$. For a system with total spin 2, there are also four channels, $^5S_2$, $^1D_2$, $^5D_2$ and $^5G_2$. And there are five channels for a $J = 3$ system, $^7S_3$, $^3D_3$, $^7D_3$, $^3G_3$ and $^7G_3$. We list all possible channels in Table 4. Their wave functions can be expressed as follows,

– For a $J = 0$ system,

$$\Psi(r,\theta,\phi)^T\chi^T_{ss_z} = \begin{bmatrix} T_S(r) \\ 0 \end{bmatrix} |^1S_0\rangle + \begin{bmatrix} 0 \\ T_D(r) \end{bmatrix} |^5D_0\rangle\,. \tag{21}$$

– For $J = 1$ system,

$$\Psi(r,\theta,\phi)^T\chi^T_{ss_z} = \begin{bmatrix} T_S(r) \\ 0 \\ 0 \\ 0 \end{bmatrix} |^3S_1\rangle + \begin{bmatrix} 0 \\ T_{D_1}(r) \\ 0 \\ 0 \end{bmatrix} |^3D_1\rangle + \begin{bmatrix} 0 \\ 0 \\ T_{D_2}(r) \\ 0 \end{bmatrix} |^7D_1\rangle + \begin{bmatrix} 0 \\ 0 \\ 0 \\ T_G(r) \end{bmatrix} |^7G_1\rangle\,. \tag{22}$$

– For a $J = 2$ system,

$$\Psi(r,\theta,\phi)^T\chi^T_{ss_z} = \begin{bmatrix} T_S(r) \\ 0 \\ 0 \\ 0 \end{bmatrix} |^5S_2\rangle + \begin{bmatrix} 0 \\ T_{D_1}(r) \\ 0 \\ 0 \end{bmatrix} |^1D_2\rangle + \begin{bmatrix} 0 \\ 0 \\ T_{D_2}(r) \\ 0 \end{bmatrix} |^5D_2\rangle + \begin{bmatrix} 0 \\ 0 \\ 0 \\ T_G(r) \end{bmatrix} |^5G_2\rangle\,. \tag{23}$$

– For a $J = 3$ system,

$$\Psi(r,\theta,\phi)^T\chi^T_{ss_z} = \begin{bmatrix} T_S(r) \\ 0 \\ 0 \\ 0 \\ 0 \end{bmatrix} |^7S_3\rangle + \begin{bmatrix} 0 \\ T_{D_1}(r) \\ 0 \\ 0 \\ 0 \end{bmatrix} |^3D_3\rangle + \begin{bmatrix} 0 \\ 0 \\ T_{D_2}(r) \\ 0 \\ 0 \end{bmatrix} |^7D_3\rangle + \begin{bmatrix} 0 \\ 0 \\ 0 \\ T_{G_1}(r) \\ 0 \end{bmatrix} |^3G_3\rangle + \begin{bmatrix} 0 \\ 0 \\ 0 \\ 0 \\ T_{G_2}(r) \end{bmatrix} |^7G_3\rangle\,. \tag{24}$$

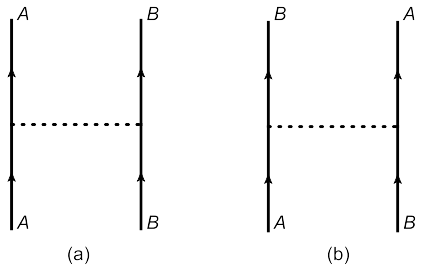


Fig. 1. Feynman diagrams for the systems composed of different baryons. "a" and "b" are direct and cross diagrams respectively.

In the expression, $\Psi(r,\theta,\phi)$ and χ_{ss_z} are the spatial and spin wave functions, respectively.

The spin of a system composed of one spin-$\frac{3}{2}$ baryon and one spin-$\frac{1}{2}$ baryon can be 1 and 2. For a $J = 1$ system, we consider the channels mixing effect between $^3S_1$, $^3D_1$ and $^5D_1$. For a system with total spin 2, there are four channels should be considered, $^5S_2$, $^3D_2$, $^5D_2$ and $^5G_2$. We also list them in Table 4. Their wave functions are the same.

The angular momentum dependent operators, Δ_{SS}, Δ_{LS} and Δ_T have different forms for various combinations

Table 3. The isospin factors for two baryon systems and baryon-antibaryon systems. The factors I_G from G-parity rule have been absorbed by the isospin factors in the right panel.

States	C_σ^s	C_π^p	C_η^p	C_K^p	C_ρ^v	C_ω^v	C_ϕ^v	$C_{K^*}^v$	States	C_σ^s	C_π^p	C_η^p	C_K^p	C_ρ^v	C_ω^v	C_ϕ^v	$C_{K^*}^v$
$[\Xi_{cc}^*\Xi_{cc}^*]^{I=0}$	1	-3/2	1/6	0	-3/2	1/2	0	0	$[\Xi_{cc}^*\bar{\Xi}_{cc}^*]^{I=0}$	1	3/2	1/6	0	-3/2	-1/2	0	0
$[\Xi_{cc}^*\Xi_{cc}^*]^{I=1}$	1	1/2	1/6	0	1/2	1/2	0	0	$[\Xi_{cc}^*\bar{\Xi}_{cc}^*]^{I=1}$	1	-1/2	1/6	0	1/2	-1/2	0	0
$[\Xi_{cc}^*\Omega_{cc}^*]^{I=\frac{1}{2}}$	1	0	-1/3	0[1]	0	0	0	0[1]	$[\Xi_{cc}^*\bar{\Omega}_{cc}^*]^{I=\frac{1}{2}}$	1	0	-1/3	0	0	0	0	0
$[\Omega_{cc}^*\Omega_{cc}^*]^{I=0}$	1	0	2/3	0	0	0	1	0	$[\Omega_{cc}^*\bar{\Omega}_{cc}^*]^{I=0}$	1	0	2/3	0	0	0	-1	0

Table 4. The channels considered in this work for two baryons systems.

	B^*B^*					B^*B			
	S	$D1$	$D2$	$G1$	$G2$	S	$D1$	$D2$	G
$J=0$	$\|^1S_0\rangle$	$\|^5D_0\rangle$							
$J=1$	$\|^3S_1\rangle$	$\|^3D_1\rangle$	$\|^7D_1\rangle$	$\|^7G_1\rangle$		$\|^3S_1\rangle$	$\|^3D_1\rangle$	$\|^5D_1\rangle$	
$J=2$	$\|^5S_2\rangle$	$\|^1D_2\rangle$	$\|^5D_2\rangle$	$\|^5G_2\rangle$		$\|^5S_2\rangle$	$\|^3D_2\rangle$	$\|^5D_2\rangle$	$\|^5G_2\rangle$
$J=3$	$\|^7S_3\rangle$	$\|^3D_3\rangle$	$\|^7D_3\rangle$	$\|^3G_3\rangle$	$\|^7G_3\rangle$				

of the baryon spins. We give their specific expressions in Table 5. We give more details about the definition of the operator matrices in Appendix B.

3 Numerical results

With the potential in Eq. (16), we solve the Schrödinger equation numerically. For the system with a binding solution, we give the binding energy ($B.E.$). The wave function of a bound state solution can also be used to check whether it is rational to treat the system as a molecular state. Using the wave function, we give the root-mean-square radius (R_{rms}),

$$R_{rms}^2 = \int \sum_i T_i^*(r) T_i(r) r^4 dr, \tag{25}$$

where T_i is the radial wave function of the ith channel. Meanwhile, we can get the individual probability for each channel,

$$P_{T_i} = \int T_i^*(r) T_i(r) r^2 dr. \tag{26}$$

In our calculation, the cutoff parameter Λ cannot be determined exactly without relevant experiment data. We treat it as a free parameter and choose different values in a reasonable range for different systems. The experience on the study of the deuteron with one-boson-exchange-potential gives us some advice. It is very successful to describe the deuteron with the cutoff between 0.8 GeV and 1.5 GeV. Since the two doubly charmed baryon system is much heavier than the deuteron, we also consider the cutoff up to 2.5 GeV.

3.1 Two spin-$\frac{3}{2}$ baryons system

For the $\Xi_{cc}^*\Xi_{cc}^*$ and $\Omega_{cc}^*\Omega_{cc}^*$ systems, we should consider the Pauli Principle. For example, the total isospin for the $\Omega_{cc}^*\Omega_{cc}^*$ system is symmetric, the total spin for the system can only be 0 and 2. For the $\Xi_{cc}^*\Omega_{cc}^*$ systems, all combinations of spin and isospin are possible. We show the binding energies and the root-mean-square radii of possible molecular states in Table 6. Because of the tensor operator, the channels with the same total angular momentum but different spin and orbital angular momenta mix each other. We also show the percentage of the different channels in the Table.

For the $J=0$ systems, we consider the $^1S_0$ and $^5D_0$ wave mixing effect. The contribution of the D-wave is actually quite small, less than 2%. For the $[\Xi_{cc}^*\Xi_{cc}^*]_{J=0}^{I=1}$ system, we find a loosely bound state with the binding energy 2.37-15.93 MeV, while the cutoff parameter is 2.0-2.4 GeV. We present the potentials of the system when the cutoff parameter is 2.2 GeV in Fig. 2, where we use V_{11}, V_{22} and V_{12} to denote the potentials for the S-wave channel, the D-wave channel, and the off-diagonal term mixing the S-wave and D-wave, respectively. The only attractive potential between the baryons appears in the S-wave. For the $[\Xi_{cc}^*\Omega_{cc}^*]_{J=0}^{I=\frac{1}{2}}$ and $[\Omega_{cc}^*\Omega_{cc}^*]_{J=0}^{I=0}$ systems, we get binding solutions when we change the cutoff parameter from 1.8 GeV to 2.2 GeV. Both of them have small binding energies and reasonable root-mean-square radii.

For the $J=1$ systems, we calculate four channel mixing effects among $^3S_1$, $^3D_1$, $^7D_1$ and $^7G_1$. Actually the contribution of G-wave almost vanishes. For the $[\Xi_{cc}^*\Xi_{cc}^*]_{J=1}^{I=0}$ system, a bound state with the binding energy 25.28-39.72 MeV appears when the cutoff parameter is chosen between 0.82-0.84 GeV. Given that the binding energy is sensitive to the cutoff parameter, and the root-mean-square radius is less than 1 fm, the system may not be a perfect candidate of the molecular state. For the $[\Xi_{cc}^*\Omega_{cc}^*]_{J=1}^{I=\frac{1}{2}}$ system, we obtain a bound state with binding energy 1.07-20.89 MeV when the cutoff parameter is 1.8-2.2 GeV. The contributions of D-wave channels increase with the cutoff parameter. The contribution of the dominant S-wave channel is 88.6% when the cutoff is 2.2 GeV.

For the $\Xi_{cc}^*\Omega_{cc}^*$ and $\Omega_{cc}^*\Omega_{cc}^*$ systems with total spin 2, we obtain binding solutions with the cutoff parameter from 2.4 GeV to 2.6 GeV. The binding solution of the former system is 1.50-11.00 MeV, and 2.71-13.03 MeV for the latter one. There is no bound state for the $[\Xi_{cc}^*\Xi_{cc}^*]_{J=2}^{I=1}$ sys-

Table 5. The specific expressions of the operators Δ_{SS}, Δ_{LS} and Δ_T for different channels. $\boldsymbol{\sigma}$ is the Pauli matrix. $\boldsymbol{S} = \frac{3}{2}\boldsymbol{\sigma}_{rs}$ is the spin operator of spin-$\frac{3}{2}$ baryons. $\boldsymbol{S}_t$ is the transition spin operator for the Rarita-Schwinger field. $\boldsymbol{L}$ is the relative orbit angular momentum operator between the two baryons. More details about the operator matrices are given in Appendix B.

Channels	Δ_{SS}	Δ_{LS}	Δ_T
$B^*B^* \to B^*B^*$	$\boldsymbol{\sigma}_{rsA}\cdot\boldsymbol{\sigma}_{rsB}$	$\frac{1}{2}\boldsymbol{L}\cdot\boldsymbol{\sigma}_{rs}$	$3\boldsymbol{\sigma}_{rsA}\cdot\hat{\boldsymbol{r}}\boldsymbol{\sigma}_{rsB}\cdot\hat{\boldsymbol{r}}-\boldsymbol{\sigma}_{rsA}\cdot\boldsymbol{\sigma}_{rsB}$
$B^*B \to B^*B$	$\boldsymbol{\sigma}_{rsA}\cdot\boldsymbol{\sigma}_{B}$	$\frac{1}{2}\boldsymbol{L}\cdot(\boldsymbol{\sigma}_{rsA}+\boldsymbol{\sigma}_{B})$	$3\boldsymbol{\sigma}_{rsA}\cdot\hat{\boldsymbol{r}}\boldsymbol{\sigma}_{B}\cdot\hat{\boldsymbol{r}}-\boldsymbol{\sigma}_{rsA}\cdot\boldsymbol{\sigma}_{B}$
$BB^* \to B^*B$	$\boldsymbol{S}^\dagger_{tA}\cdot\boldsymbol{S}_{tB}$	$\frac{1}{2}\boldsymbol{L}\cdot\left(\boldsymbol{S}^\dagger_{tA}+\boldsymbol{S}_{tB}\right)$	$3\boldsymbol{S}^\dagger_{tA}\cdot\hat{\boldsymbol{r}}\boldsymbol{S}_{tB}\cdot\hat{\boldsymbol{r}}-\boldsymbol{S}^\dagger_{tA}\cdot\boldsymbol{S}_{tB}$
$B^*B \to B^*B^*$	$\boldsymbol{\sigma}_{rsA}\cdot\boldsymbol{S}^\dagger_{tB}$	$\frac{1}{2}\boldsymbol{L}\cdot\left(\boldsymbol{\sigma}_{rsA}+\boldsymbol{S}^\dagger_{tB}\right)$	$3\boldsymbol{\sigma}_{rsA}\cdot\hat{\boldsymbol{r}}\boldsymbol{S}^\dagger_{tB}\cdot\hat{\boldsymbol{r}}-\boldsymbol{\sigma}_{rsA}\cdot\boldsymbol{S}^\dagger_{tB}$
$B^*B \to BB$	$\boldsymbol{S}_{tA}\cdot\boldsymbol{\sigma}_{B}$	$\frac{1}{2}\boldsymbol{L}\cdot(\boldsymbol{S}_{tA}+\boldsymbol{\sigma}_{B})$	$3\boldsymbol{S}_{tA}\cdot\hat{\boldsymbol{r}}\boldsymbol{\sigma}_{B}\cdot\hat{\boldsymbol{r}}-\boldsymbol{S}_{tA}\cdot\boldsymbol{\sigma}_{B}$
$BB \to BB$	$\boldsymbol{\sigma}_{A}\cdot\boldsymbol{\sigma}_{B}$	$\frac{1}{2}\boldsymbol{L}\cdot\boldsymbol{\sigma}$	$3\boldsymbol{\sigma}_{A}\cdot\hat{\boldsymbol{r}}\boldsymbol{\sigma}_{B}\cdot\hat{\boldsymbol{r}}-\boldsymbol{\sigma}_{A}\cdot\boldsymbol{\sigma}_{B}$

tem, even if we include the couple-channel effect and vary the cutoff parameter from 0.8 GeV to 3 GeV. The relevant interaction potentials with the cutoff parameter 1.0 GeV is shown in Fig. 3. The S-wave and D-wave potentials of the system, V_{11}, V_{22} and V_{33}, are hardly attractive.

For the $J = 3$ case, there are only two possible systems, $[\Xi^*_{cc}\Xi^*_{cc}]^{I=0}_{J=3}$ and $[\Xi^*_{cc}\Omega^*_{cc}]^{I=\frac{1}{2}}_{J=3}$. We consider the mixing effect of five channels, $^7S_3$, $^3D_3$, $^7D_3$, $^3G_3$ and $^7G_3$. The binding energy of the $[\Xi^*_{cc}\Xi^*_{cc}]^{I=0}_{J=3}$ system is 2.65-8.87 MeV, when we change the cut off from 1.2 GeV to 1.4 GeV. The contribution of the channel $^7D_3$ is important, the percentage of which is over 10%. For the $[\Xi^*_{cc}\Omega^*_{cc}]^{I=\frac{1}{2}}_{J=3}$ system, the binding energy changes from 8.39 MeV to 25.78 MeV while the cutoff parameter changes from 1.12 GeV to 1.16 GeV. In the wave functions, the S-wave is dominant, whose contribution is over 99%. The root-mean-square radius of the bound state is 0.64-1.02 fm, which seems a little small for a loosely bound state composed of two doubly charmed baryons.

Among all possible systems composed of two spin-$\frac{3}{2}$ baryons, the systems $[\Xi^*_{cc}\Xi^*_{cc}]^{I=1}_{J=0,3}$, $[\Xi^*_{cc}\Omega^*_{cc}]^{I=\frac{1}{2}}_{J=0,1,2}$ and $[\Omega^*_{cc}\Omega^*_{cc}]^{I=0}_{J=0,2}$ are good candidates of molecular states. For the system $[\Xi^*_{cc}\Xi^*_{cc}]^{I=0}_{J=1}$ and $[\Xi^*_{cc}\Omega^*_{cc}]^{I=\frac{1}{2}}_{J=3}$, the existence of the bound solutions is very sensitive to cutoff parameter. Meanwhile, their root-mean-square radii are less than 1fm. We do not find a binding solution for the $[\Xi^*_{cc}\Xi^*_{cc}]^{I=1}_{J=2}$ system.

3.2 One spin-$\frac{3}{2}$ baryon and one spin-$\frac{1}{2}$ baryon system

We investigate the possible molecular systems composed of one spin-$\frac{3}{2}$ baryon and one spin-$\frac{1}{2}$ baryon. Their total spin can be 1 and 2. For the $J = 1$ system, we consider the couple-channel effect among $^3S_1$, $^3D_1$ and $^5D_1$ channels. For the $J = 2$ system, the couple-channel effect is among $^5S_2$, $^3D_2$, $^5D_2$ and $^5G_2$ channels. We show the binding energies, root-mean-square radii and contributions of different channels of the $\Xi^*_{cc}\Xi_{cc}$ and $\Omega^*_{cc}\Omega_{cc}$ systems in Table 7.

For the $[\Xi^*_{cc}\Xi_{cc}]^{I=0}_{J=1}$ system, we obtain a loosely bound state with binding energy 4.73-12.57 MeV while the cutoff parameter is 1.2-1.6 GeV. The D-wave contribution is about 10% and decreases as the cutoff parameter increases. For the $[\Xi^*_{cc}\Xi_{cc}]^{I=1}_{J=1}$ system, the contribution of the S-wave is over 99%. When we choose the cutoff parameter at 1.05 GeV, the binding energy of the bound state is 8.34 MeV. For the $[\Omega^*_{cc}\Omega_{cc}]^{I=0}_{J=1}$ system, we find a bound state solution with binding energy 8.97 while the cutoff parameter is 1.25 GeV. For the $[\Omega^*_{cc}\Xi_{cc}]^{I=1/2}_{J=1}$ system, a bound solution with a dominant S-wave appears when the cutoff is 1.2 GeV-1.3 GeV. The result of $[\Xi^*_{cc}\Omega_{cc}]^{I=1/2}_{J=1}$ is very similar to that of $[\Omega^*_{cc}\Xi_{cc}]^{I=1/2}_{J=1}$. The two systems are related by the U-spin and the V-spin symmetry.

For the systems with total spin 2, the contributions of the G-wave channels are almost zero. For the $[\Xi^*_{cc}\Xi_{cc}]^{I=0}_{J=2}$ system, a loosely bound state with binding energy 2.33-10.15 MeV appears when the cutoff parameter is 1.2-1.6 GeV. The contribution of $^5D_2$ is about 8% when the cutoff is 1.4 GeV. For the $[\Xi^*_{cc}\Xi_{cc}]^{I=1}_{J=2}$ system, we obtain a binding solution with the binding energy 8.78 MeV while the cutoff parameter is 1.05 GeV. In the system, the D-waves contributions are less than 1%. For the $[\Omega^*_{cc}\Omega_{cc}]^{I=0}_{J=2}$ system, we obtain a binding solution with the binding energy 9.19 MeV when we choose the cutoff parameter as 1.25 GeV. The D-waves contributions are also very small. The results for $[\Omega^*_{cc}\Xi_{cc}]^{I=1/2}_{J=2}$ and $[\Xi^*_{cc}\Omega_{cc}]^{I=1/2}_{J=2}$ are almost the same. When we choose the cutoff from 1.0 GeV to 1.1 GeV, we find a bound state with binding energy 3.68-42.66 MeV for the former system, and a binding solution with binding energy 1.53-32.4 MeV for the latter one.

Considering the reasonable binding energies and root-mean-square-radii of the above solutions, the spin-$\frac{3}{2}$ baryon and spin-$\frac{1}{2}$ baryon systems are all good candidates of molecular states.

3.3 The two doubly charmed systems with multi-channel mixing effect

We calculate the systems with channel mixing among BB, B^*B and B^*B^* in this subsection. B and B^* are the spin-$\frac{1}{2}$ and spin-$\frac{3}{2}$ doubly charmed baryons, respectively. We present the possible systems with certain total spin and isospin in Tables 8-10. In the previous subsection, the couple-channel effect from the high angular momentum

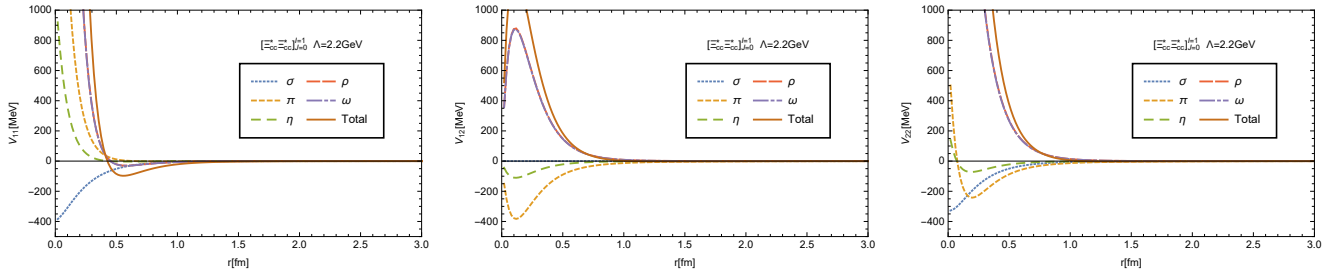
Table 6. The numerical results for the B^*B^* systems. Λ is the cutoff parameter. "$B.E.$" is the binding energy. R_{rms} is the root-mean-square radius. P_i is the percentage of the different channels.

States	Λ(MeV)	E(MeV)	R_{rms}(fm)	P_S(%)	P_{D1}(%)	P_{D2}(%)	P_{G1}(%)	P_{G2}(%)
$[\Xi^*_{cc}\Xi^*_{cc}]^{I=1}_{J=0}$	2000	2.37	2.15	99.5	0.5			
	2200	7.46	1.45	98.9	1.1			
	2400	15.93	1.17	97.9	2.1			
$[\Xi^*_{cc}\Omega^*_{cc}]^{I=\frac{1}{2}}_{J=0}$	1800	1.11	2.75	99.8	0.2			
	2000	5.19	1.60	99.3	0.7			
	2200	12.93	1.22	98.5	1.5			
$[\Omega^*_{cc}\Omega^*_{cc}]^{I=0}_{J=0}$	1800	1.12	2.66	99.9	0.1			
	2000	5.50	1.50	99.6	0.4			
	2200	14.20	1.14	98.9	1.1			
$[\Xi^*_{cc}\Xi^*_{cc}]^{I=0}_{J=1}$	800	25.28	0.99	94.4	5.2	0.4	0.0	
	820	31.66	0.91	94.3	5.4	0.3	0.0	
	840	39.72	0.84	94.2	5.5	0.3	0.0	
$[\Xi^*_{cc}\Omega^*_{cc}]^{I=\frac{1}{2}}_{J=1}$	1800	1.07	2.90	97.9	2.1	0.0	0.0	
	2000	7.47	1.59	93.2	6.7	0.1	0.0	
	2200	20.89	1.25	88.6	11.1	0.3	0.0	
$[\Xi^*_{cc}\Xi^*_{cc}]^{I=1}_{J=2}$				×				
$[\Xi^*_{cc}\Omega^*_{cc}]^{I=\frac{1}{2}}_{J=2}$	2400	1.50	2.43	95.6	0.4	3.9	0.1	
	2500	5.04	1.62	91.9	0.7	7.2	0.2	
	2600	11.00	1.31	88.4	1.0	10.3	0.3	
$[\Omega^*_{cc}\Omega^*_{cc}]^{I=0}_{J=2}$	2400	2.71	1.92	95.8	0.4	3.7	0.1	
	2500	6.70	1.45	93.0	0.7	6.2	0.1	
	2600	13.03	1.21	90.0	0.9	8.9	0.2	
$[\Xi^*_{cc}\Xi^*_{cc}]^{I=0}_{J=3}$	1200	2.65	2.86	89.7	0.3	9.9	0.0	0.1
	1300	5.29	2.34	88.5	0.3	11.0	0.0	0.2
	1400	8.87	2.01	88.1	0.2	11.4	0.0	0.3
$[\Xi^*_{cc}\Omega^*_{cc}]^{I=\frac{1}{2}}_{J=3}$	1120	8.39	1.02	99.7	0.0	0.3	0.0	0.0
	1140	15.43	0.79	99.5	0.0	0.4	0.0	0.1
	1160	25.78	0.64	99.2	0.0	0.7	0.0	0.1

states are small. The components of G-wave in the total wave functions are usually negligible. Thus we only consider the D-wave in our calculation.

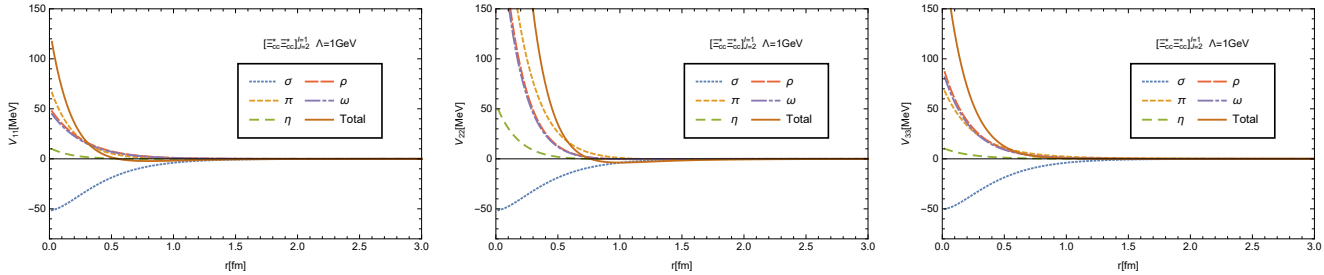
Because the masses of various systems are different, we define the binding energy relative to the BB threshold. When we solve the coupled Schrödinger equations, we put the mass difference in the kinetic term. The effective potentials as well as the spin and orbital angular momentum dependent operators are consistent with what we defined before. However, we ignore the spin-orbital coupling effect in the off-diagonal elements of the interaction potentials. Because the effect is dependent on the external momentum, we can treat it as a high order correction compared with spin-spin and tensor interactions. Thus, it is reasonable to use only spin-spin and tensor interactions to describe the channel mixing effect. The numerical results including binding energies, root-mean-square radii and percentages of different channels are shown in Tables 11-13.

For the $\Omega^{(*)}_{cc}\Omega^{(*)}_{cc}$ system with $I(J^P) = 0(0^+)$, we find a binding solution when the cutoff is around 1.3 GeV. The dominant component of this solution is $\Omega_{cc}\Omega_{cc}|^1S_0\rangle$. The component of $\Omega^*_{cc}\Omega^*_{cc}|^1S_0\rangle$ increases with the cutoff parameter. The D-wave contributions to the system are insignificant. For the system with $I(J^P) = 0(2^+)$, we find a solution with the main component $\Omega_{cc}\Omega^*_{cc}|^5S_2\rangle$, which



(a) V_{11} (b) V_{12} (c) V_{22}

Fig. 2. The interactions potentials for the system $[\Xi_{cc}^*\Xi_{cc}^*]_{J=0}^{I=1}$. V_{11}, V_{12} and V_{22} denote the ${}^1S_0 \leftrightarrow {}^1S_0$, ${}^1S_0 \leftrightarrow {}^5D_0$ and ${}^5D_0 \leftrightarrow {}^5D_0$ transitions potentials.



(a) V_{11} (b) V_{22} (c) V_{33}

Fig. 3. The interactions potentials for the system $[\Xi_{cc}^*\Xi_{cc}^*]_{J=2}^{I=1}$. V_{11}, V_{22} and V_{33} denote the diagonal terms in the potential matrix for the channels ${}^5S_2$, ${}^1D_2$ and ${}^5D_2$ respectively.

agrees with the single channel results in subsection 3.2. The mixing effect of the channel $\Omega_{cc}^*\Omega_{cc}^*|{}^5S_2\rangle$ is about 10% and should not be ignored.

For the $\Xi_{cc}^{(*)}\Xi_{cc}^{(*)}$ system with $I(J^P) = 0(1^+)$, we find a binding solution with a small cutoff, 0.8 GeV. The channel mixing effect is very prominent among the $\Xi_{cc}\Xi_{cc}$, $\Xi_{cc}^*\Xi_{cc}^*$ and $\Xi_{cc}\Xi_{cc}^*$ with S-wave. Their contributions to the total wave function are about 50%, 35% and 15%, respectively. The D-wave channels mixing effect in this system is tiny. For the $I(J^P) = 0(3^+)$ system, the channel mixing effect is also important. We obtain a binding solution with cutoff around 1.38 GeV. In the system, it is interesting that the D-wave contribution of $\Xi_{cc}\Xi_{cc}^*$ reaches up to 28%. For the $I(J^P) = 1(0^+)$ system, a binding solution with the main channel $\Xi_{cc}\Xi_{cc}|{}^1S_0\rangle$ appears when the cutoff is 1.06 GeV. For the $I(J^P) = 1(2^+)$ system, we obtain a binding solution based on $\Xi_{cc}\Xi_{cc}^*|{}^3S_1\rangle$. The result is consistent with the calculation considering only the couple-channel effect inside the $\Xi_{cc}\Xi_{cc}^*$ systems. The $\Xi_{cc}^*\Xi_{cc}^*$ channels contribute 7%-10% to the wave function, which makes the cutoff parameter a little larger when the binding energy is the same.

The isospin of the $\Xi_{cc}^{(*)}\Omega_{cc}^{(*)}$ systems is $\frac{1}{2}$. For the system with $J = 0$, we find a bound state with binding energy 1.21-28.64 MeV. The 97% component of the system is the $\Xi_{cc}\Omega_{cc}|{}^3S_0\rangle$ state when the cutoff is 1.17 GeV. The main part of the rest components is the S-wave of $\Xi_{cc}^*\Omega_{cc}^*$. For the $I(J^P) = \frac{1}{2}(1^+)$ system, we obtain a binding solution when the cutoff is around 1.2 GeV. The system has a main part of the $\Xi_{cc}\Omega_{cc}|{}^1S_0\rangle$ channel, which mixes with the channel $\Xi_{cc}^*\Omega_{cc}^*|{}^1S_0\rangle$. For the system with $J = 2$, a bound state solution appears when the cutoff is 1.1 GeV. The system is dominated by the S-waves of $\Xi_{cc}^*\Omega_{cc}$ and $\Xi_{cc}\Omega_{cc}^*$, and their contributions are 56.2% and 43.5%, respectively. For the system with $I(J^P) = \frac{1}{2}(3^+)$, we obtain a binding solution when the cutoff is around 1.3 GeV. In this system, the contribution of the $\Xi_{cc}^*\Omega_{cc}^*|{}^7S_3\rangle$ channel is over 93%, which is the only possible S-wave channel. The main component of the other channels are the $|{}^5D_3\rangle$ states of $\Xi_{cc}^*\Omega_{cc}$ and $\Xi_{cc}\Omega_{cc}^*$, each of which has the contribution about 2.7%.

In Ref. [34], the authors studied the systems composed of two spin-$\frac{1}{2}$ doubly charmed baryons. We show the results in Table 14 and make some comparison. After considering the channel mixing effect among the BB, B^*B and B^*B^* systems, we get some different conclusions for the $0(0^+)$, $1(0^+)$ and $\frac{1}{2}(0^+)$ systems. As an example, we show the potentials of the $0(0^+)$ systems in Fig. 4, where we give the potentials of the main channels. In the single channel calculation Ref. [34], the attraction of the $\Omega_{cc}\Omega_{cc}$ system is too weak to produce a bound state. But with the help of the channel mixing effects, especially the $\Omega_{cc}^*\Omega_{cc}^*|{}^1S_0\rangle$ channel, we can obtain a binding solution. The channel mixing effect plays the same role for the $1(0^+)$ and $\frac{1}{2}(0^+)$ systems.

Most of the $B^{(*)}B^{(*)}$ systems with the channel mixing effect are dominated by one channel with the percentage about 90%. However, the couple-channel effect from other channels may produce a bound state, which does not exist in the single channel case. Another interesting observation

Table 7. The numerical results for the B^*B systems. Λ is the cutoff parameter. "$B.E.$" is the binding energy. R_{rms} is the root-mean-square radius. P_i is the percentage of the different channels.

States	Λ(MeV)	E(MeV)	R_{rms}(fm)	P_S(%)	P_{D1}(%)	P_{D2}(%)	P_F(%)
$[\Xi_{cc}^*\Xi_{cc}]_{J=1}^{I=0}$	1200	4.73	2.56	87.3	6.1	6.6	
	1400	8.29	2.15	88.0	5.4	6.6	
	1600	12.57	1.86	90.2	4.3	5.5	
$[\Xi_{cc}^*\Xi_{cc}]_{J=1}^{I=1}$	1000	1.85	2.17	98.9	0.6	0.5	
	1050	8.34	1.11	99.5	0.3	0.2	
	1100	24.39	0.67	99.9	0.1	0.0	
$[\Omega_{cc}^*\Omega_{cc}]_{J=1}^{I=0}$	1200	3.01	1.64	99.5	0.3	0.2	
	1250	8.97	1.03	99.6	0.2	0.2	
	1300	22.34	0.69	99.98	0.1	0.1	
$[\Omega_{cc}^*\Xi_{cc}]_{J=1}^{I=1/2}$	1200	4.36	1.48	99.3	0.6	0.1	
	1250	9.68	1.06	99.5	0.4	0.1	
	1300	18.74	0.79	99.8	0.2	0.0	
$[\Xi_{cc}^*\Omega_{cc}]_{J=1}^{I=1/2}$	1200	2.68	1.77	99.5	0.4	0.1	
	1250	6.81	1.19	99.6	0.3	0.1	
	1300	14.24	0.87	99.8	0.2	0.0	
$[\Xi_{cc}^*\Xi_{cc}]_{J=2}^{I=0}$	1200	2.33	2.89	91.4	0.5	8.1	0.0
	1400	5.66	2.19	91.2	0.5	8.3	0.0
	1600	10.15	1.80	92.6	0.4	7.0	0.0
$[\Xi_{cc}^*\Xi_{cc}]_{J=2}^{I=1}$	1000	1.91	2.06	99.2	0.0	0.8	0.0
	1050	8.78	1.05	99.6	0.0	0.4	0.0
	1100	25.32	0.64	99.9	0.0	0.1	0.0
$[\Omega_{cc}^*\Omega_{cc}]_{J=2}^{I=0}$	1200	2.97	1.62	99.6	0.0	0.4	0.0
	1250	9.19	1.00	99.7	0.0	0.3	0.0
	1300	23.06	0.67	99.9	0.0	0.1	0.0
$[\Omega_{cc}^*\Xi_{cc}]_{J=2}^{I=1/2}$	1000	3.68	1.54	99.4	0.3	0.3	0.0
	1050	16.00	0.86	99.5	0.2	0.3	0.0
	1100	42.66	0.72	99.7	0.21	0.2	0.0
$[\Xi_{cc}^*\Omega_{cc}]_{J=2}^{I=1/2}$	1000	1.53	2.17	99.6	0.2	0.2	0.0
	1050	10.47	0.99	99.6	0.2	0.2	0.0
	1100	32.40	0.64	99.7	0.2	0.1	0.0

Table 8. Possible mixing channels for the $\Omega_{cc}^{(*)}\Omega_{cc}^{(*)}$ system with $J = 0$ and $J = 2$.

$I(J^P)$	$\Omega_{cc}\Omega_{cc}$	$\Omega_{cc}^*\Omega_{cc}^*$	$\Omega_{cc}\Omega_{cc}^*$
$0(0^+)$	$\|^1S_0\rangle$	$\|^1S_0\rangle$ $\|^5D_0\rangle$	$\|^5D_0\rangle$
$0(2^+)$	$\|^1D_2\rangle$	$\|^5S_2\rangle$ $\|^1D_2\rangle$ $\|^5D_2\rangle$	$\|^5S_2\rangle$ $\|^3D_2\rangle$ $\|^5D_2\rangle$

is that the two or three main components of the systems are comparable, which may cause a large shift of the binding energy. Actually the numerical results are quite complicated with the couple-channel effect. The binding solutions become even more sensitive to the cutoff parameter.

4 Discussions and conclusions

In this work, with the help of the one-boson-exchange model, we systematically investigate the possible molecular systems composed of two spin-$\frac{3}{2}$ doubly charmed baryons,

Table 9. Possible mixing channels for the $\Xi_{cc}^{(*)}\Xi_{cc}^{(*)}$ system with total angular momentum 0, 1, 2 and 3.

$I(J^P)$	$\Xi_{cc}\Xi_{cc}$	$\Xi_{cc}^*\Xi_{cc}^*$	$\Xi_{cc}\Xi_{cc}^*$
$0(1^+)$	$\|^3S_1\rangle$ $\|^3D_1\rangle$	$\|^3S_1\rangle$ $\|^3D_1\rangle$ $\|^7D_1\rangle$	$\|^3S_1\rangle$ $\|^3D_1\rangle$ $\|^5D_1\rangle$
$0(3^+)$	$\|^3D_3\rangle$	$\|^7S_3\rangle$ $\|^3D_3\rangle$ $\|^7D_3\rangle$	$\|^3D_3\rangle$ $\|^5D_3\rangle$
$1(0^+)$	$\|^1S_0\rangle$	$\|^1S_0\rangle$ $\|^5D_0\rangle$	$\|^5D_0\rangle$
$1(2^+)$	$\|^1D_2\rangle$	$\|^5S_2\rangle$ $\|^1D_2\rangle$ $\|^5D_2\rangle$	$\|^5S_2\rangle$ $\|^3D_2\rangle$ $\|^5D_2\rangle$

Table 10. Possible mixing channels for the $\Xi_{cc}^{(*)}\Omega_{cc}^{(*)}$ system with total angular momentum 0, 1, 2 and 3.

$I(J^P)$	$\Xi_{cc}\Omega_{cc}$	$\Xi_{cc}^*\Omega_{cc}^*$	$\Xi_{cc}^*\Omega_{cc}$	$\Xi_{cc}\Omega_{cc}^*$
$\frac{1}{2}(0^+)$	$\|^1S_0\rangle$	$\|^1S_0\rangle$ $\|^5D_0$	$\|^5D_0\rangle$	$\|^5D_0\rangle$
$\frac{1}{2}(1^+)$	$\|^3S_1\rangle$ $\|^3D_1\rangle$	$\|^3S_1\rangle$ $\|^3D_1\rangle$ $\|^7D_1\rangle$	$\|^3S_1\rangle$ $\|^3D_1\rangle$ $\|^5D_1\rangle$	$\|^3S_1\rangle$ $\|^3D_1\rangle$ $\|^5D_1\rangle$
$\frac{1}{2}(2^+)$	$\|^1D_2\rangle$	$\|^5S_2\rangle$ $\|^1D_2\rangle$ $\|^5D_2\rangle$	$\|^5S_2\rangle$ $\|^3D_2\rangle$ $\|^5D_2\rangle$	$\|^5S_2\rangle$ $\|^3D_2\rangle$ $\|^5D_2\rangle$
$\frac{1}{2}(3^+)$	$\|^3D_3\rangle$	$\|^7S_3\rangle$ $\|^3D_3\rangle$ $\|^7D_3\rangle$	$\|^3D_3\rangle$ $\|^5D_3\rangle$	$\|^3D_3\rangle$ $\|^5D_3\rangle$

Table 11. The numerical results for the $\Omega^{(*)}\Omega^{(*)}$ systems. Λ is the cutoff parameter. "$B.E.$" is the binding energy. R_{rms} is the root-mean-square radius.

$I(J^P)$	Result			$\Omega_{cc}\Omega_{cc}$	$\Omega_{cc}^*\Omega_{cc}^*$			$\Omega_{cc}\Omega_{cc}^*$		
$0(0^+)$	Λ(MeV)	B.E.(MeV)	R_{rms}(fm)	$\|^1S_0\rangle$	$\|^1S_0\rangle$	$\|^5D_0\rangle$		$\|^5D_0\rangle$		
	1300	5.64	1.34	94.8	4.1	0.1		1.0		
	1350	21.69	0.84	87.1	10.8	0.1		2.0		
	1400	57.81	0.61	78.9	18.5	0.0		2.6		
$0(2^+)$	Λ(MeV)	B.E.(MeV)	R_{rms}(fm)	$\|^1D_2\rangle$	$\|^5S_2\rangle$	$\|^1D_2\rangle$	$\|^5D_2\rangle$	$\|^5S_2\rangle$	$\|^3D_2\rangle$	$\|^5D_2\rangle$
	1360	10.24	0.50	0.6	6.5	0.1	0.4	92.4	0.0	0.0
	1370	28.92	0.47	0.5	7.7	0.1	0.4	91.2	0.0	0.0
	1380	49.90	0.45	0.5	8.9	0.1	0.4	90.1	0.0	0.0

B^*B^*, as well as the systems composed of one spin-$\frac{3}{2}$ and one spin-$\frac{1}{2}$ doubly charmed baryon, B^*B. We also study the couple-channel effect between various combinations of baryons. We consider the S-waves and D-waves of the BB, B^*B^* and BB^* systems together. The binding energies are defined relative to the BB threshold, and the mass differences of different channels are put in the kinetic terms when calculating the coupled Schrödinger equations.

For the two spin-$\frac{3}{2}$ doubly charmed baryons systems, we consider the channels mixing among possible S-wave D-wave and G-wave. After considering the binding energies and root-mean-square radii, as well as the reasonable value of cutoff parameter, the following systems are good candidate of molecular states, $[\Xi_{cc}^*\Xi_{cc}^*]_{J=0,3}^{I=1}$, $[\Xi_{cc}^*\Omega_{cc}^*]_{J=0,1,2}^{I=\frac{1}{2}}$ and $[\Omega_{cc}^*\Omega_{cc}^*]_{J=0,2}^{I=0}$.

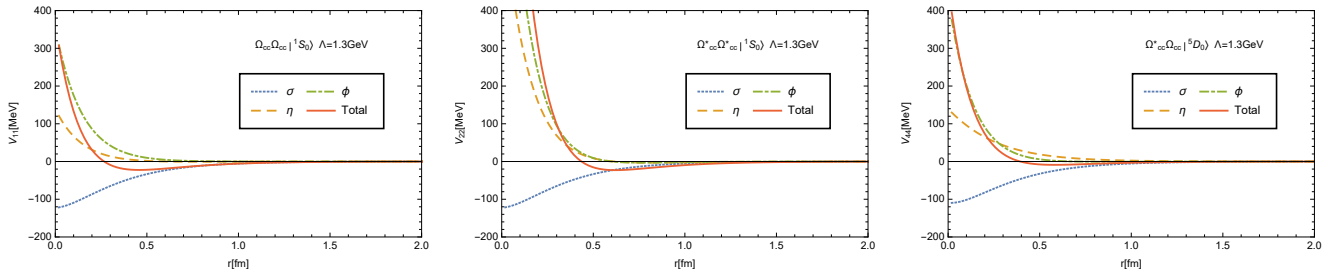
For the system composed of one spin-$\frac{3}{2}$ baryon and one spin-$\frac{1}{2}$ baryon, their total spin can be 1 or 2. We consider the channels mixing among $^3S_1$, $^3D_1$, $^5D_1$ for the $J=1$ system. For the system with $J=2$, we consider the channels mixing between $^5S_2$, $^3D_2$, $^5D_2$ and $^5G_2$. The spin-$\frac{3}{2}$ baryon and spin-$\frac{1}{2}$ baryon systems are all candidates of molecular states, such as $[\Xi_{cc}^*\Xi_{cc}]_{J=1,2}^{I=0,1}$, $[\Omega_{cc}^*\Omega_{cc}]_{J=1,2}^{I=0}$ and $[\Xi_{cc}^*\Omega_{cc}(\Omega_{cc}^*\Xi_{cc})]_{J=1,2}^{I=\frac{1}{2}}$. The systems $[\Xi_{cc}^*\Xi_{cc}]_{J=1,2}^{I=0}$ are particularly interesting. Both of them have small binding energies around several MeVs, and large root-mean-square radii, 2-3 fm, when the cutoff is from 1.2 GeV to 1.6 GeV.

We also consider the channel mixing between the S-wave and D-wave BB, B^*B^* and BB^* states. Most of the $B^{(*)}B^{(*)}$ systems are dominated by one single channel, which has about 90% contribution. However, the channel mixing effect from the other channels may produce a bound state, which does not exist in the single channel case, such as the systems with $J=0$. Moreover, the two or three main components of the systems are sometimes comparable, which may cause a large shift of the binding energy, such as the system with $I(J^P)=0(1^+)$.

As a byproduct, we consider the systems composed of one baryon and one antibaryon, $B^*\bar{B}^*$ and $B^*\bar{B}$. The results are collected in Appendix C. The baryon-antibaryon systems may not be stable, because of the three meson decay modes through quark rearrangement when the threshold is open. Although molecular states composed of two doubly charmed baryons seem too hard to be produced in

Table 12. The numerical results for the $\Xi^{(*)}\Xi^{(*)}$ systems. Λ is the cutoff parameter. "$B.E.$" is the binding energy. R_{rms} is the root-mean-square radius.

$I(J^P)$	Result			$\Xi_{cc}\Xi_{cc}$		$\Xi^*_{cc}\Xi^*_{cc}$			$\Xi_{cc}\Xi^*_{cc}$		
$0(1^+)$	Λ(MeV)	B.E.(MeV)	R_{rms}(fm)	$\vert^3S_1\rangle$	$\vert^3D_1\rangle$	$\vert^3S_1\rangle$	$\vert^3D_1\rangle$	$\vert^7D_1\rangle$	$\vert^3S_1\rangle$	$\vert^3D_1\rangle$	$\vert^5D_1\rangle$
	800	36.47	1.01	52.9	0.0	31.9	0.0	0.2	14.4	0.1	0.5
	810	42.61	0.96	50.8	0.0	33.9	0.0	0.2	14.5	0.1	0.5
	820	49.34	0.92	49.0	0.0	35.9	0.0	0.1	14.5	0.0	0.5
$0(3^+)$	Λ(MeV)	B.E.(MeV)	R_{rms}(fm)	$\vert^3D_3\rangle$		$\vert^7S_3\rangle$	$\vert^3D_3\rangle$	$\vert^7D_3\rangle$	$\vert^3D_3\rangle$	$\vert^5D_3\rangle$	
	1370	5.50	1.35	0.4		58.4	0.8	0.9	11.3	28.2	
	1380	11.01	1.32	0.4		58.2	0.9	0.9	11.3	28.4	
	1400	22.69	1.23	0.5		57.4	1.2	1.1	11.2	28.6	
$1(0^+)$	Λ(MeV)	B.E.(MeV)	R_{rms}(fm)	$\vert^1S_0\rangle$		$\vert^1S_0\rangle$	$\vert^5D_0\rangle$		$\vert^5D_0\rangle$		
	1060	0.87	2.91	95.9		3.0	0.1		1.0		
	1100	8.83	1.21	86.4		10.8	0.1		2.7		
	1150	35.62	0.78	76.5		19.7	0.1		3.7		
$1(2^+)$	Λ(MeV)	B.E.(MeV)	R_{rms}(fm)	$\vert^1D_2\rangle$		$\vert^5S_2\rangle$	$\vert^1D_2\rangle$	$\vert^5D_2\rangle$	$\vert^5S_2\rangle$	$\vert^3D_2\rangle$	$\vert^5D_2\rangle$
	1120	13.26	0.58	0.7		6.7	0.2	0.4	92.0	0.0	0.0
	1130	29.16	0.54	0.6		8.0	0.2	0.4	90.8	0.0	0.0
	1140	47.10	0.51	0.5		9.4	0.2	0.4	89.5	0.0	0.0



(a) V_{11} (b) V_{22} (c) V_{44}

Fig. 4. The interactions potentials for the system with$I(J^P) = 0(0^+)$. V_{11}, V_{22} and V_{44} denote the diagonal terms in the potential matrix for the channels $\Omega_{cc}\Omega_{cc}|^1S_0\rangle$, $\Omega^*_{cc}\Omega^*_{cc}|^1S_0\rangle$ and $\Omega^*_{cc}\Omega_{cc}|^5D_0\rangle$ respectively.

the experiment, some possible structure composed of one baryon and one antibaryon may be discovered at LHCb in the future if they are not very broad.

Acknowledgements: B. Yang is very grateful to X.Z Weng and G.J. Wang for very helpful discussions. This project is supported by the National Natural Science Foundation of China under Grants 11575008, 11621131001 and National Key Basic Research Program of China (2015CB856700).

Table 13. The numerical results for the $\Xi^{(*)}\Omega^{(*)}$ systems. Λ is the cutoff parameter. "$B.E.$" is the binding energy. R_{rms} is the root-mean-square radius.

$I(J^P)$	Result			$\Xi_{cc}\Omega_{cc}$		$\Xi^*_{cc}\Omega^*_{cc}$			$\Xi^*_{cc}\Omega_{cc}$			$\Xi_{cc}\Omega^*_{cc}$		
$\frac{1}{2}(0^+)$	Λ(MeV)	B.E.(MeV)	R_{rms}(fm)	$\|^1S_0\rangle$		$\|^1S_0\rangle$	$\|^5D_0\rangle$		$\|^5D_0\rangle$			$\|^5D_0\rangle$		
	1170	1.21	2.50	97.0		2.3	0.0		0.3			0.3		
	1200	5.98	1.35	92.0		6.5	0.0		0.8			0.7		
	1250	28.64	0.81	81.7		15.7	0.0		1.3			1.3		
$\frac{1}{2}(1^+)$	Λ(MeV)	B.E.(MeV)	R_{rms}(fm)	$\|^3S_1\rangle$	$\|^3D_1\rangle$	$\|^3S_1\rangle$	$\|^3D_1\rangle$	$\|^7D_1\rangle$	$\|^3S_1\rangle$	$\|^3D_1\rangle$	$\|^5D_1\rangle$	$\|^3S_1\rangle$	$\|^3D_1\rangle$	$\|^5D_1\rangle$
	1200	5.97	1.38	93.4	0.0	5.1	0.0	0.1	0.3	0.1	0.4	0.2	0.1	0.4
	1220	12.05	1.10	90.2	0.0	7.8	0.0	0.0	0.4	0.2	0.5	0.2	0.2	0.5
	1240	21.11	0.94	87.0	0.0	10.7	0.0	0.0	0.4	0.3	0.6	0.3	0.2	0.5
$\frac{1}{2}(2^+)$	Λ(MeV)	B.E.(MeV)	R_{rms}(fm)	$\|^1D_2\rangle$		$\|^5S_2\rangle$	$\|^1D_2\rangle$	$\|^5D_2\rangle$	$\|^5S_2\rangle$	$\|^3D_2\rangle$	$\|^5D_2\rangle$	$\|^5S_2\rangle$	$\|^3D_2\rangle$	$\|^5D_2\rangle$
	1080	2.24	0.67	0.0		0.0	0.0	0.0	59.0	0.2	0.0	40.7	0.1	0.0
	1100	29.0	0.59	0.0		0.0	0.0	0.0	56.2	0.2	0.0	43.5	0.1	0.0
	1120	61.28	0.54	0.0		0.0	0.0	0.0	54.3	0.1	0.0	45.5	0.1	0.0
$\frac{1}{2}(3^+)$	Λ(MeV)	B.E.(MeV)	R_{rms}(fm)	$\|^3D_3\rangle$		$\|^7S_3\rangle$	$\|^3D_3\rangle$	$\|^7D_3\rangle$	$\|^3D_3\rangle$	$\|^5D_3\rangle$		$\|^3D_3\rangle$	$\|^5D_3\rangle$	
	1290	7.28	0.55	0.0		93.76	0.0	0.0	0.4	2.8		0.4	2.8	
	1300	23.69	0.53	0.0		93.97	0.0	0.0	0.4	2.7		0.4	2.7	
	1310	41.13	0.51	0.1		93.8	0.0	0.0	0.4	2.6		0.4	2.7	

Table 14. The comparison of the BB systems with and without channel mixing effect for the systems B^*B^* and B^*B.

	This work			[34]		
$I(J^P)$	Λ(MeV)	B.E.(MeV)	R_{rms}(fm)	Λ(MeV)	B.E.(MeV)	R_{rms}(fm)
$\frac{1}{2}(1^+)$	1200	5.97	1.38	1200	0.56	3.45
$0(1^+)$	800	36.47	1.01	1100	0.68	3.32
$0(0^+)$	1300	5.64	1.34		×	
$1(0^+)$	1060	0.87	2.91		×	
$\frac{1}{2}(0^+)$	1170	1.21	2.50		×	

A Fourier transformation formulae

The specific expressions of the scalar functions $H_i = H_i(\Lambda, m_{\sigma/\alpha/\beta}, r)$ and $M_i = M_i(\Lambda, m_\alpha, r)$ are as follows,

$$\begin{aligned}
H_0(\Lambda,m,r) &= Y(ur) - \tfrac{\lambda}{u}Y(\lambda r) - \tfrac{r\beta^2}{2u}Y(\lambda r),\\
H_1(\Lambda,m,r) &= Y(ur) - \tfrac{\lambda}{u}Y(\lambda r) - \tfrac{r\lambda^2\beta^2}{2u^3}Y(\lambda r),\\
H_2(\Lambda,m,r) &= Z_1(ur) - \tfrac{\lambda^3}{u^3}Z_1(\lambda r) - \tfrac{\lambda\beta^2}{2u^3}Y(\lambda r),\\
H_3(\Lambda,m,r) &= Z(ur) - \tfrac{\lambda^3}{u^3}Z(\lambda r) - \tfrac{\lambda\beta^2}{2u^3}Z_2(\lambda r),\\
M_0(\Lambda,m,r) &= -\tfrac{1}{\theta r}\left[\cos(\theta r) - e^{-\lambda r}\right] + \tfrac{\beta^2}{2\theta\lambda}e^{-\lambda r},\\
M_1(\Lambda,m,r) &= -\tfrac{1}{\theta r}\left[\cos(\theta r) - e^{-\lambda r}\right] - \tfrac{\lambda\beta^2}{2\theta^3}e^{-\lambda r},\\
M_3(\Lambda,m,r) &= -\left[\cos(\theta r) - \tfrac{3\sin(\theta r)}{\theta r} - 3\tfrac{\cos(\theta r)}{\theta^2 r^2}\right]\tfrac{1}{\theta r}\\
&\quad -\tfrac{\lambda^3}{\theta^3}Z(\lambda r) - \tfrac{\lambda\beta^2}{2\theta^3}Z_2(\lambda r),
\end{aligned} \tag{27}$$

where

$$\beta^2 = \Lambda^2 - m^2, \quad u^2 = m^2 - Q_0^2,$$

$$\theta^2 = -(m^2 - Q_0^2), \quad \lambda^2 = \Lambda^2 - Q_0^2,$$

and

$$Y(x) = \frac{e^{-x}}{x}, \quad Z(x) = (1 + \frac{3}{x} + \frac{3}{x^2})Y(x),$$

$$Z_1(x) = (\frac{1}{x} + \frac{1}{x^2})Y(x), \quad Z_2(x) = (1+x)Y(x).$$

Q_0 in the expression is the zeroth component of the four momentum of exchanged meson.

The above scalar functions come from Fourier transformation. We give some useful Fourier transformation for-

mulae.

$$\begin{aligned}
\frac{1}{u^2+\boldsymbol{Q}^2}\mathcal{F}^2(Q) &\to \tfrac{u}{4\pi}H_0(\Lambda,m,r),\\
\frac{\boldsymbol{Q}^2}{u^2+\boldsymbol{Q}^2}\mathcal{F}^2(Q) &\to -\tfrac{u^3}{4\pi}H_1(\Lambda,m,r),\\
\frac{\boldsymbol{Q}}{u^2+\boldsymbol{Q}^2}\mathcal{F}^2(Q) &\to \tfrac{iu^3}{4\pi}\boldsymbol{r}H_2(\Lambda,m,r),\\
\frac{Q_iQ_j}{u^2+\boldsymbol{Q}^2}\mathcal{F}^2(Q) &\to -\tfrac{u^3}{12\pi}[H_3(\Lambda,m,r)K_{ij}\\
&\quad + H_1(\Lambda,m,r)\delta_{ij}].
\end{aligned} \tag{28}$$

If $u_{ex}^2 = m_{ex}^2 - Q_0^2 < 0$, the last formula above changes into

$$\begin{aligned}
\frac{Q_iQ_j}{u^2+\boldsymbol{Q}^2}\mathcal{F}^2(Q) \to -\frac{\theta^3}{12\pi}&[M_3(\Lambda,m,r)K_{ij}\\
&+ M_1(\Lambda,m,r)\delta_{ij}].
\end{aligned} \tag{29}$$

B Operators

We extract some specific structures in the effective potentials and express them as some angular momentum dependent operators, Δ_{SS}, Δ_{LS} and Δ_T. For the system with spin-$\frac{1}{2}$ initial and final states, their structures are as follows,

$$\begin{aligned}
\Delta_{S_AS_B} = \boldsymbol{\sigma}\cdot\boldsymbol{\sigma},\ \Delta_{LS} = \boldsymbol{L}\cdot\boldsymbol{S},\\
\Delta_T = \tfrac{3\boldsymbol{\sigma}\cdot\boldsymbol{r}\boldsymbol{\sigma}\cdot\boldsymbol{r}}{r^2} - \boldsymbol{\sigma}\cdot\boldsymbol{\sigma},
\end{aligned} \tag{30}$$

where $\boldsymbol{L}$ and $\boldsymbol{S}$ are the orbital angular momentum and total spin of two baryons. $\boldsymbol{\sigma}$ is the Pauli matrix.

For a spin-$\frac{3}{2}$ baryon, we introduce the Rarita-Schwinger field Ψ^μ. The field is defined through

$$\Psi^\mu(\lambda) = \sum_{m_\lambda}\sum_{m_s}\langle 1m_\lambda,\frac{1}{2}m_s|\frac{3}{2}\rangle\,\epsilon^\mu(m_\lambda)\chi(m_s) = S_t^\mu\Phi(\lambda), \tag{31}$$

where $\chi(m_s)$ is a two-component spinor with the third component of spin m_s. $\epsilon^\mu(m_\lambda)$ is the polarization vector of a $J=1$ field with the third component of spin m_λ,

$$\begin{aligned}
\epsilon^\mu(+) &= -\frac{1}{\sqrt{2}}[0,1,i,0]^T,\ \epsilon^\mu(0) = [0,0,0,1]^T,\\
\epsilon^\mu(-) &= \frac{1}{\sqrt{2}}[0,1,-i,0]^T.
\end{aligned} \tag{32}$$

$\Phi(\lambda)$ is the eigenfunction of the spin operator of a spin-$\frac{3}{2}$ baryons.

$$\begin{aligned}
\Phi\left(\frac{3}{2}\right) &= [1,0,0,0]^T,\ \Phi\left(\frac{1}{2}\right) = [0,1,0,0]^T,\\
\Phi\left(-\frac{1}{2}\right) &= [0,0,1,0]^T,\ \Phi\left(-\frac{3}{2}\right) = [0,0,0,1]^T.
\end{aligned} \tag{33}$$

With the above specific form, we can obtain the transition operator S_t^μ.

$$\begin{aligned}
S_t^0 =&0,\ S_t^x = \frac{1}{\sqrt{2}}\begin{bmatrix}-1 & 0 & \frac{1}{\sqrt{3}} & 0\\ 0 & -\frac{1}{\sqrt{3}} & 0 & 1\end{bmatrix},\\
S_t^y =&-\frac{i}{\sqrt{2}}\begin{bmatrix}1 & 0 & \frac{1}{\sqrt{3}} & 0\\ 0 & \frac{1}{\sqrt{3}} & 0 & 1\end{bmatrix},\ S_t^x = \begin{bmatrix}0 & \sqrt{\frac{2}{3}} & 0 & 0\\ 0 & 0 & \sqrt{\frac{2}{3}} & 0\end{bmatrix}.
\end{aligned} \tag{34}$$

The spin operator for the spin-$\frac{3}{2}$ particles can be derived as $\boldsymbol{S} = \frac{3}{2}\boldsymbol{\sigma}_{rs}$, while $\boldsymbol{\sigma}_{rs} \equiv -S_{t\mu}^\dagger\boldsymbol{\sigma}S_t^\mu$.

C Numerical results of the baryon-antibaryon system

We calculate the possible molecular states formed by one baryon and one antibaryon. Although the baryon-antibaryon systems may be not stable, we give the possible molecular solutions for reference.

C.1 The $B^*\bar{B}^*$ system

We calculate the systems composed of one spin-$\frac{3}{2}$ baryon and one spin-$\frac{3}{2}$ antibaryon. For the $\Xi_{cc}^*\bar{\Omega}_{cc}^*$ and $\bar{\Xi}_{cc}^*\Omega_{cc}^*$ systems, they are antiparticles of each other and we only calculate the former system. We show the binding energies and the root-mean-square radii of possible molecular states in Tables 15 and 16. The mixing channels are the same as those for the two spin-$\frac{3}{2}$ baryons systems. Therefore, the angular momentum dependent operators are also the same.

For the $\left[\Xi_{cc}^*\bar{\Xi}_{cc}^*\right]_{J=0}^{I=0}$ system, we find a binding solution with binding energy 1.96-8.78 MeV when we choose the cutoff parameter between 0.94 GeV and 0.98 GeV. The D-wave contribution is significant and increases with the cutoff parameter. When we choose the cutoff around 1.0 GeV, the percentage of the ${}^5D_0$ channel is over 30%. We give the interaction potentials of the system in Fig. 5. If only the S-wave is considered, the barely attractive potential could not produce a bound state. But the couple-channel effect from an adequately attractive D-wave makes it possible. For the $\left[\Xi_{cc}^*\bar{\Xi}_{cc}^*\right]_{J=0}^{I=1}$ system, the binding energy is 2.68-14.88 MeV while the cutoff is 1.0-1.2 GeV. For the $\left[\Xi_{cc}^*\bar{\Omega}_{cc}^*\right]_{J=0}^{I=\frac{1}{2}}$ system, we obtain a bound state. The binding energy of the system is 12.54 MeV when the cutoff parameter is 1.5 GeV. Although the root-mean-square radius of the system is 0.76fm when we choose a large cutoff parameter, the system still seems to be a molecular states with the cutoff parameter less than 1.5 GeV. For the $\left[\Omega_{cc}^*\bar{\Omega}_{cc}^*\right]_{J=0}^{I=0}$ system, a binding solution with the binding energy 1.48-27.87 MeV appears with the cutoff parameter from 1.25 GeV to 1.35 GeV.

For the $\left[\Xi_{cc}^*\bar{\Xi}_{cc}^*\right]_{J=1}^{I=0}$ system, we obtain a bound state with the binding energy 1.63-27.92 MeV while the cutoff parameter is 0.9-1.0 GeV. The G-wave contribution of

Table 15. The numerical results for the $B^*\bar{B}^*$ systems with $J = 0, 1$. Λ is the cutoff parameter. "$B.E.$" is the binding energy. R_{rms} is the root-mean-square radius. P_i is the percentage of the different channels.

States	Λ(MeV)	$B.E.$(MeV)	R_{rms}(fm)	P_S(%)	P_{D1}(%)	P_{D2}(%)	P_G(%)
$\left[\Xi^*_{cc}\bar{\Xi}^*_{cc}\right]^{I=0}_{J=0}$	940	1.96	2.96	81.9	18.1		
	960	4.45	2.28	75.7	24.3		
	980	8.78	1.85	70.5	29.5		
$\left[\Xi^*_{cc}\bar{\Xi}^*_{cc}\right]^{I=1}_{J=0}$	1000	2.68	1.82	99.3	0.7		
	1100	7.63	1.22	99.2	0.8		
	1200	14.88	0.95	99.1	0.9		
$\left[\Xi^*_{cc}\bar{\Omega}^*_{cc}\right]^{I=\frac{1}{2}}_{J=0}$	1400	6.40	1.19	99.7	0.3		
	1500	12.54	0.92	99.6	0.4		
	1600	20.92	0.76	99.5	0.5		
$\left[\Omega^*_{cc}\bar{\Omega}^*_{cc}\right]^{I=0}_{J=0}$	1250	1.48	2.32	98.5	1.5		
	1300	8.62	1.21	96.1	3.9		
	1350	27.87	0.81	93.9	6.1		
$\left[\Xi^*_{cc}\bar{\Xi}^*_{cc}\right]^{I=0}_{J=1}$	900	1.63	3.26	85.9	8.4	5.7	0.0
	950	9.52	2.01	74.6	14.3	11.0	0.1
	1000	27.92	1.52	67.7	16.6	15.6	0.1
$\left[\Xi^*_{cc}\bar{\Xi}^*_{cc}\right]^{I=1}_{J=1}$	1000	1.07	2.71	99.0	0.8	0.2	0.0
	1200	9.98	1.17	98.2	1.6	0.2	0.0
	1400	27.05	0.82	97.6	2.1	0.3	0.0
$\left[\Xi^*_{cc}\bar{\Omega}^*_{cc}\right]^{I=\frac{1}{2}}_{J=1}$	1400	4.18	1.44	99.7	0.2	0.1	0.0
	1500	8.69	1.09	99.5	0.4	0.1	0.0
	1600	14.97	0.89	99.3	0.6	0.1	0.0
$\left[\Omega^*_{cc}\bar{\Omega}^*_{cc}\right]^{I=0}_{J=1}$	1250	1.67	2.26	98.5	1.0	0.5	0.0
	1300	7.01	1.37	96.5	2.3	1.2	0.0
	1350	18.68	1.02	94.4	3.4	2.2	0.0

the system is almost zero. However, the total contribution of the $^3D_1$ and $^7D_1$ channel is about 30%. For the other three systems with total spin 1, $\left[\Xi^*_{cc}\bar{\Xi}^*_{cc}\right]^{I=1}_{J=1}$, $\left[\Xi^*_{cc}\bar{\Omega}^*_{cc}\right]^{I=\frac{1}{2}}_{J=1}$ and $\left[\Omega^*_{cc}\bar{\Omega}^*_{cc}\right]^{I=0}_{J=1}$, we all find binding solutions with reasonable binding energies and root-mean-square radii. The dominant parts of their wave functions are all S-wave.

For the systems $\left[\Xi^*_{cc}\bar{\Xi}^*_{cc}\right]^{I=0}_{J=2}$, a bound state appears with binding energy about 1.15 MeV, when the cutoff parameter is around 0.95 GeV. The D-waves are important for the system. The contribution of the $^5D_2$ channel is almost 10% when the cutoff parameter is 0.95 GeV. For the $\left[\Xi^*_{cc}\bar{\Xi}^*_{cc}\right]^{I=1}_{J=2}$, $\left[\Xi^*_{cc}\bar{\Omega}^*_{cc}\right]^{I=\frac{1}{2}}_{J=2}$ and $\left[\Omega^*_{cc}\bar{\Omega}^*_{cc}\right]^{I=0}_{J=2}$ systems, each of them has a loosely bound state solution, and dominant S-wave part in the total wave function. We show the binding energies, root-mean-square radii as well as the contributions of all the channels in the Table 16.

For the $\left[\Xi^*_{cc}\bar{\Xi}^*_{cc}\right]^{I=0}_{J=3}$ system, we obtain a bound state with binding energy 7.26-36.68 MeV when the cutoff varies from 0.8 GeV to 1.0 GeV. For the $\left[\Xi^*_{cc}\bar{\Xi}^*_{cc}\right]^{I=1}_{J=3}$ system, the loosely bound state solution appears until we change the cutoff parameter over 2.0 GeV. We change the cutoff parameter from 2.2 GeV to 2.6 GeV, and the binding energy increases from 2.16 MeV to 5.78 MeV. For the $\left[\Xi^*_{cc}\bar{\Omega}^*_{cc}\right]^{I=\frac{1}{2}}_{J=3}$ system, we find a binding solution with binding energy 1.69-5.53 MeV when the cutoff parameter is 1.8-2.2 GeV. The binding energies of the above two systems are stable for the cutoff parameter in the range over 2.0 GeV. For the $\left[\Omega^*_{cc}\bar{\Omega}^*_{cc}\right]^{I=0}_{J=3}$ system, a bound state with binding energy 1.15-14.06 MeV appears when the cutoff parameter changes from 1.2 GeV to 1.4 GeV.

For the possible systems composed of one spin-$\frac{3}{2}$ baryon and one spin-$\frac{3}{2}$ antibaryon, they are all good candidates of molecular states. A baryon-antibaryon system may be unstable especially when the threshold of three mesons is open. Some of these molecular systems may appear as an

Table 16. The numerical results for the $B^*\bar{B}^*$ systems with $J = 2, 3$. Λ is the cutoff parameter. "$B.E.$" is the binding energy. R_{rms} is the root-mean-square radius. P_i is the percentage of the different channels.

States	Λ(MeV)	$B.E.$(MeV)	R_{rms}(fm)	P_S(%)	P_{D1}(%)	P_{D2}(%)	P_{G1}(%)	P_{G2}(%)
$\left[\Xi^*_{cc}\bar{\Xi}^*_{cc}\right]^{I=0}_{J=2}$	900	1.15	3.39	92.4	1.9	5.7	0.0	
	950	6.50	2.00	87.4	3.0	9.5	0.1	
	1000	18.13	1.51	83.9	3.8	12.1	0.2	
$\left[\Xi^*_{cc}\bar{\Xi}^*_{cc}\right]^{I=1}_{J=2}$	1400	3.80	1.69	98.3	0.2	1.5	0.0	
	1600	10.21	1.18	97.8	0.2	2.0	0.0	
	1800	19.13	0.94	97.2	0.3	2.5	0.0	
$\left[\Xi^*_{cc}\bar{\Omega}^*_{cc}\right]^{I=\frac{1}{2}}_{J=2}$	1600	4.31	1.46	99.6	0.1	0.3	0.0	
	1800	9.93	1.07	99.3	0.1	0.6	0.0	
	2000	17.62	0.87	98.9	0.1	1.0	0.0	
$\left[\Omega^*_{cc}\bar{\Omega}^*_{cc}\right]^{I=0}_{J=2}$	1300	4.64	1.55	97.9	0.4	1.7	0.0	
	1400	18.22	1.04	94.8	1.2	4.0	0.0	
	1500	45.21	0.84	90.9	2.3	6.7	0.1	
$\left[\Xi^*_{cc}\bar{\Xi}^*_{cc}\right]^{I=0}_{J=3}$	800	7.26	1.59	96.7	0.7	2.5	0.0	0.1
	900	17.90	1.29	94.7	1.2	3.9	0.0	0.2
	1000	36.68	1.19	89.2	2.4	8.0	0.1	0.3
$\left[\Xi^*_{cc}\bar{\Xi}^*_{cc}\right]^{I=1}_{J=3}$	2200	2.16	2.27	96.9	0.2	2.9	0.0	0.0
	2400	3.76	1.86	96.1	0.3	3.6	0.0	0.0
	2600	5.78	1.59	95.3	0.3	4.4	0.0	0.0
$\left[\Xi^*_{cc}\bar{\Omega}^*_{cc}\right]^{I=\frac{1}{2}}_{J=3}$	1800	1.69	2.21	99.4	0.1	0.5	0.0	0.0
	2000	3.32	1.71	99.0	0.1	0.9	0.0	0.0
	2200	5.33	1.45	98.5	0.1	1.4	0.0	0.0
$\left[\Omega^*_{cc}\bar{\Omega}^*_{cc}\right]^{I=0}_{J=3}$	1200	1.15	2.56	99.3	0.1	0.6	0.0	0.0
	1300	5.06	1.53	97.6	0.4	2.0	0.0	0.0
	1400	14.06	1.17	94.5	0.9	4.6	0.0	0.0

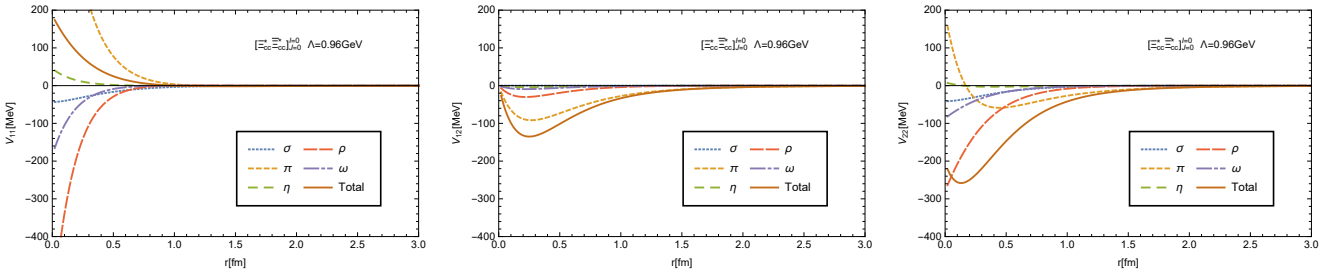
enhancement in the baryon and antibaryon invariant mass spectrum, or a narrow resonance state etc.

C.2 The $B^*\bar{B}$ system

We also consider the systems composed of one spin-$\frac{3}{2}$ baryon and one spin-$\frac{1}{2}$ antibaryon, $B^*\bar{B}$. The mixing channels are the same as that for the two baryon systems with the same total angular momentum. The numerical results are shown in Table 17.

For the $\left[\Xi^*_{cc}\bar{\Xi}_{cc}\right]^{I=0}_{J=1}$ system, we find a bound state with binding energy 1.67-18.21 MeV when the cutoff parameter is 0.9-1.1 GeV. For the $\left[\Xi^*_{cc}\bar{\Xi}_{cc}\right]^{I=1}_{J=1}$ system, a very loosely bound state solution with binding energy 2.96 MeV appears with the cutoff parameter is 2.5 GeV. The bound state is quite insensitive to the cutoff parameter. The D-wave contribution is very small. For the $\left[\Xi^*_{cc}\bar{\Omega}_{cc}\right]^{I=\frac{1}{2}}_{J=1}$ system, we find a binding solution insensitive to the cutoff parameter. The binding energy increases from 1.82 MeV to 8.06 MeV along with the cutoff parameter changing from 1.8 GeV to 2.6 GeV. The $\left[\Omega^*_{cc}\bar{\Xi}_{cc}\right]^{I=\frac{1}{2}}_{J=1}$ system is quite similar to the $\left[\Xi^*_{cc}\bar{\Omega}_{cc}\right]^{I=\frac{1}{2}}_{J=1}$ system. A bound state with binding energy 1.86-8.15 MeV appears with the same range of the cutoff parameter. It is not surprising because the $\left[\Omega^*_{cc}\bar{\Xi}_{cc}\right]^{I=\frac{1}{2}}_{J=1}$ state and the $\left[\bar{\Xi}^*_{cc}\Omega_{cc}\right]^{I=\frac{1}{2}}_{J=1}$ state are degenerate in the heavy quark limit. For the $\left[\Omega^*_{cc}\bar{\Omega}_{cc}\right]^{I=0}_{J=1}$ system, we obtain a binding solution with binding energy 1.78-19.23 MeV when the cutoff parameter is 1.3-1.7 GeV. The S-wave contribution is 99%.

The G-wave contributions for the $J = 2$ systems are negligible. The contributions of D-waves are also very small. For the $\left[\Xi^*_{cc}\bar{\Xi}_{cc}\right]^{I=0}_{J=2}$ system, we obtain a binding solution with binding energy 2.52-26.29 MeV when we choose the cutoff parameter from 1.0 GeV to 1.08 GeV. For the $\left[\Xi^*_{cc}\bar{\Xi}_{cc}\right]^{I=1}_{J=2}$ system, we find a loosely bound



(a) V_{11} (b) V_{12} (c) V_{22}

Fig. 5. The interactions potentials for the system $[\Xi_{cc}^*\Xi_{cc}^*]_{J=2}^{I=1}$. V_{11}, V_{12} and V_{22} denote the ${}^1S_0 \leftrightarrow {}^1S_0$, ${}^1S_0 \leftrightarrow {}^5D_0$ and ${}^5D_0 \leftrightarrow {}^5D_0$ transitions potentials.

state. When the cutoff parameter changes from 1.4 GeV to 1.8 GeV, the binding energy increases from 1.78 MeV to 11.66 MeV. For the $\left[\Xi_{cc}^*\bar{\Omega}_{cc}\right]_{J=2}^{I=\frac{1}{2}}$ and $\left[\Omega_{cc}^*\bar{\Xi}_{cc}\right]_{J=2}^{I=\frac{1}{2}}$ systems, we obtain binding solutions when the cutoff parameter changes from 1.5 GeV to 1.9 GeV. The binding energy of the $\Xi_{cc}^*\bar{\Omega}_{cc}$ system is 1.70-10.26 MeV, while that of the $\Omega_{cc}^*\bar{\Xi}_{cc}$ system is 1.74-10.38 MeV. For the $\left[\Omega_{cc}^*\bar{\Omega}_{cc}\right]_{J=2}^{I=0}$ system, a bound state with binding energy 2.55-30.91 MeV appears when the cutoff parameter is 1.3-1.5 GeV.

For the four $J=1$ systems, $\left[\Xi_{cc}^*\bar{\Xi}_{cc}\right]_{J=1}^{I=1}$, $\left[\Xi_{cc}^*\bar{\Omega}_{cc}\right]_{J=1}^{I=\frac{1}{2}}$, $\left[\Omega_{cc}^*\bar{\Xi}_{cc}\right]_{J=1}^{I=\frac{1}{2}}$ and $\left[\Omega_{cc}^*\bar{\Omega}_{cc}\right]_{J=1}^{I=0}$, their loosely bound solutions are very insensitive to the cutoff parameter.

References

1. S. K. Choi et al. Observation of a narrow charmonium - like state in exclusive B+- —¿ K+- pi+ pi- J / psi decays. *Phys. Rev. Lett.*, 91:262001, 2003.
2. Z. Q. Liu et al. Study of $e^+e^{-+-}J/$ and Observation of a Charged Charmoniumlike State at Belle. *Phys. Rev. Lett.*, 110:252002, 2013.
3. M. Ablikim et al. Observation of a Charged Charmonium-like Structure in e^+e^{-} $^{+-}$ J/ at $\sqrt{s}$ =4.26 GeV. *Phys. Rev. Lett.*, 110:252001, 2013.
4. T. Xiao, S. Dobbs, A. Tomaradze, and Kamal K. Seth. Observation of the Charged Hadron $Z_c^{\pm}(3900)$ and Evidence for the Neutral $Z_c^0(3900)$ in $e^+e^- \to \pi\pi J/\psi$ at $\sqrt{s} = 4170$ MeV. *Phys. Lett.*, B727:366–370, 2013.
5. Bernard Aubert et al. Observation of a broad structure in the $\pi^+\pi^- J/\psi$ mass spectrum around 4.26-GeV/c^2. *Phys. Rev. Lett.*, 95:142001, 2005.
6. Q. He et al. Confirmation of the Y(4260) resonance production in ISR. *Phys. Rev.*, D74:091104, 2006.
7. T. Aaltonen et al. Evidence for a Narrow Near-Threshold Structure in the $J/\psi\phi$ Mass Spectrum in $B^+ \to J/\psi\phi K^+$ Decays. *Phys. Rev. Lett.*, 102:242002, 2009.
8. A. Bondar et al. Observation of two charged bottomonium-like resonances in Y(5S) decays. *Phys. Rev. Lett.*, 108:122001, 2012.
9. Roel Aaij et al. Observation of $J/\psi p$ Resonances Consistent with Pentaquark States in $\Lambda_b^0 \to J/\psi K^- p$ Decays. *Phys. Rev. Lett.*, 115:072001, 2015.
10. Roel Aaij et al. Observation of a narrow pentaquark state, $P_c(4312)^+$, and of two-peak structure of the $P_c(4450)^+$. *Phys. Rev. Lett.*, 122:222001, 2019.
11. Hua-Xing Chen, Wei Chen, Xiang Liu, and Shi-Lin Zhu. The hidden-charm pentaquark and tetraquark states. *Phys. Rept.*, 639:1–121, 2016.
12. A. Esposito, A. Pilloni, and A. D. Polosa. Multiquark Resonances. *Phys. Rept.*, 668:1–97, 2017.
13. Hua-Xing Chen, Wei Chen, Xiang Liu, Yan-Rui Liu, and Shi-Lin Zhu. A review of the open charm and open bottom systems. *Rept. Prog. Phys.*, 80(7):076201, 2017.
14. Richard F. Lebed, Ryan E. Mitchell, and Eric S. Swanson. Heavy-Quark QCD Exotica. *Prog. Part. Nucl. Phys.*, 93:143–194, 2017.
15. Feng-Kun Guo, Christoph Hanhart, Ulf-G. Meiner, Qian Wang, Qiang Zhao, and Bing-Song Zou. Hadronic molecules. *Rev. Mod. Phys.*, 90(1):015004, 2018.

Table 17. The numerical results for the $B^*\bar{B}$ systems. Λ is the cutoff parameter. "$B.E.$" is the binding energy. R_{rms} is the root-mean-square radius. P_i is the percentage of the different channels.

States	Λ(MeV)	$B.E.$(MeV)	R_{rms}(fm)	P_S(%)	P_{D1}(%)	P_{D2}(%)	P_G(%)
$\left[\Xi_{cc}^*\bar{\Xi}_{cc}\right]_{J=1}^{I=0}$	900	1.67	2.21	99.8	0.1	0.1	
	1000	8.82	1.24	99.6	0.2	0.2	
	1100	18.21	1.03	99.3	0.4	0.3	
$\left[\Xi_{cc}^*\bar{\Xi}_{cc}\right]_{J=1}^{I=1}$	2500	2.96	1.79	99.3	0.1	0.6	
	3000	5.68	1.39	99.0	0.1	0.9	
	3500	8.67	1.19	98.7	0.1	1.2	
$\left[\Xi_{cc}^*\bar{\Omega}_{cc}\right]_{J=1}^{I=\frac{1}{2}}$	1800	1.82	2.06	99.9	0.0	0.1	
	2200	4.86	1.39	99.8	0.0	0.2	
	2600	8.06	1.15	99.7	0.0	0.3	
$\left[\Omega_{cc}^*\bar{\Xi}_{cc}\right]_{J=1}^{I=\frac{1}{2}}$	1800	1.86	2.05	99.9	0.0	0.1	
	2200	4.93	1.39	99.8	0.0	0.2	
	2600	8.15	1.15	99.7	0.0	0.3	
$\left[\Omega_{cc}^*\bar{\Omega}_{cc}\right]_{J=1}^{I=0}$	1300	1.78	2.09	99.8	0.0	0.2	
	1500	8.32	1.22	99.1	0.0	0.9	
	1700	19.23	0.97	97.6	0.1	2.3	
$\left[\Xi_{cc}^*\bar{\Xi}_{cc}\right]_{J=2}^{I=0}$	1000	2.52	2.26	96.3	0.9	2.8	0.0
	1040	10.77	1.39	94.6	1.3	4.1	0.0
	1080	26.29	1.04	93.7	1.4	4.9	0.0
$\left[\Xi_{cc}^*\bar{\Xi}_{cc}\right]_{J=2}^{I=1}$	1400	1.78	2.17	99.6	0.1	0.3	0.0
	1600	5.88	1.36	99.4	0.2	0.4	0.0
	1800	11.66	1.05	99.2	0.3	0.5	0.0
$\left[\Xi_{cc}^*\bar{\Omega}_{cc}\right]_{J=2}^{I=\frac{1}{2}}$	1500	1.70	2.10	99.9	0.0	0.1	0.0
	1700	5.26	1.32	99.8	0.1	0.1	0.0
	1900	10.26	1.02	99.7	0.1	0.2	0.0
$\left[\Omega_{cc}^*\bar{\Xi}_{cc}\right]_{J=2}^{I=\frac{1}{2}}$	1500	1.74	2.08	99.9	0.0	0.1	0.0
	1700	5.34	1.32	99.8	0.1	0.1	0.0
	1900	10.38	1.02	99.7	0.1	0.2	0.0
$\left[\Omega_{cc}^*\bar{\Omega}_{cc}\right]_{J=2}^{I=0}$	1300	2.55	1.83	99.6	0.1	0.3	0.0
	1400	11.71	1.05	98.8	0.3	0.9	0.0
	1500	30.91	0.77	97.8	0.5	1.7	0.0

16. Stephen Lars Olsen, Tomasz Skwarnicki, and Daria Zieminska. Nonstandard heavy mesons and baryons: Experimental evidence. *Rev. Mod. Phys.*, 90(1):015003, 2018.
17. Chang-Zheng Yuan. The XYZ states revisited. *Int. J. Mod. Phys.*, A33(21):1830018, 2018.
18. Yan-Rui Liu, Hua-Xing Chen, Wei Chen, Xiang Liu, and Shi-Lin Zhu. Pentaquark and Tetraquark states. 2019.
19. M. B. Voloshin and L. B. Okun. Hadron Molecules and Charmonium Atom. *JETP Lett.*, 23:333–336, 1976. [Pisma Zh. Eksp. Teor. Fiz.23,369(1976)].
20. A. De Rujula, Howard Georgi, and S. L. Glashow. Molecular Charmonium: A New Spectroscopy? *Phys. Rev. Lett.*, 38:317, 1977.
21. Nils A. Tornqvist. From the deuteron to deusons, an analysis of deuteron - like meson meson bound states. *Z. Phys.*, C61:525–537, 1994.
22. Nils A. Tornqvist. On deusons or deuteron - like meson meson bound states. *Nuovo Cim.*, A107:2471–2476, 1994.
23. Cheuk-Yin Wong. Molecular states of heavy quark mesons. *Phys. Rev.*, C69:055202, 2004.

24. Xiang Liu and Shi-Lin Zhu. Y(4143) is probably a molecular partner of Y(3930). *Phys. Rev.*, D80:017502, 2009. [Erratum: Phys. Rev.D85,019902(2012)].
25. Frank Close and Clark Downum. On the possibility of Deeply Bound Hadronic Molecules from single Pion Exchange. *Phys. Rev. Lett.*, 102:242003, 2009.
26. Gui-Jun Ding, Jia-Feng Liu, and Mu-Lin Yan. Dynamics of Hadronic Molecule in One-Boson Exchange Approach and Possible Heavy Flavor Molecules. *Phys. Rev.*, D79:054005, 2009.
27. Zhi-Feng Sun, Jun He, Xiang Liu, Zhi-Gang Luo, and Shi-Lin Zhu. $Z_b(10610)^{\pm}$ and $Z_b(10650)^{\pm}$ as the $B^*\bar{B}$ and $B^*\bar{B}^*$ molecular states. *Phys. Rev.*, D84:054002, 2011.
28. Ning Li, Zhi-Feng Sun, Xiang Liu, and Shi-Lin Zhu. Coupled-channel analysis of the possible $D^{(*)}D^{(*)}, \overline{B}^{(*)}\overline{B}^{(*)}$ and $D^{(*)}\overline{B}^{(*)}$ molecular states. *Phys. Rev.*, D88(11):114008, 2013.
29. Lu Zhao, Li Ma, and Shi-Lin Zhu. Spin-orbit force, recoil corrections, and possible $B\bar{B}^*$ and $D\bar{D}^*$ molecular states. *Phys. Rev.*, D89(9):094026, 2014.
30. Ning Lee, Zhi-Gang Luo, Xiao-Lin Chen, and Shi-Lin Zhu. Possible Deuteron-like Molecular States Composed of Heavy Baryons. *Phys. Rev.*, D84:014031, 2011.
31. Wakafumi Meguro, Yan-Rui Liu, and Makoto Oka. Possible $\Lambda_c\Lambda_c$ molecular bound state. *Phys. Lett.*, B704:547–550, 2011.
32. Ning Li and Shi-Lin Zhu. Hadronic Molecular States Composed of Heavy Flavor Baryons. *Phys. Rev.*, D86:014020, 2012.
33. T. F. Carames and A. Valcarce. Heavy flavor dibaryons. *Phys. Rev.*, D92(3):034015, 2015.
34. Lu Meng, Ning Li, and Shi-Lin Zhu. Deuteron-like states composed of two doubly charmed baryons. *Phys. Rev.*, D95(11):114019, 2017.
35. Lu Meng, Ning Li, and Shi-lin Zhu. Possible hadronic molecules composed of the doubly charmed baryon and nucleon. *Eur. Phys. J.*, A54(9):143, 2018.
36. Bin Yang, Lu Meng, and Shi-Lin Zhu. Hadronic molecular states composed of spin- $\frac{3}{2}$ singly charmed baryons. *Eur. Phys. J.*, A55(2):21, 2019.
37. Jia-Jun Wu, R. Molina, E. Oset, and B. S. Zou. Prediction of narrow N^* and Λ^* resonances with hidden charm above 4 GeV. *Phys. Rev. Lett.*, 105:232001, 2010.
38. Zhong-Cheng Yang, Zhi-Feng Sun, Jun He, Xiang Liu, and Shi-Lin Zhu. The possible hidden-charm molecular baryons composed of anti-charmed meson and charmed baryon. *Chin. Phys.*, C36:6–13, 2012.
39. Rui Chen, Xiang Liu, Xue-Qian Li, and Shi-Lin Zhu. Identifying exotic hidden-charm pentaquarks. *Phys. Rev. Lett.*, 115(13):132002, 2015.
40. L. Roca, J. Nieves, and E. Oset. LHCb pentaquark as a $\bar{D}^*\Sigma_c - \bar{D}^*\Sigma_c^*$ molecular state. *Phys. Rev.*, D92(9):094003, 2015.
41. Yasuhiro Yamaguchi, Alessandro Giachino, Atsushi Hosaka, Elena Santopinto, Sachiko Takeuchi, and Makoto Takizawa. Hidden-charm and bottom meson-baryon molecules coupled with five-quark states. *Phys. Rev.*, D96(11):114031, 2017.
42. Yuki Shimizu and Masayasu Harada. Hidden Charm Pentaquark $P_c(4380)$ and Doubly Charmed Baryon $\Xi_{cc}^*(4380)$ as Hadronic Molecule States. *Phys. Rev.*, D96(9):094012, 2017.
43. Yasuhiro Yamaguchi and Elena Santopinto. Hidden-charm pentaquarks as a meson-baryon molecule with coupled channels for $\bar{D}^{(*)}\Lambda_c$ and $\bar{D}^{(*)}\Sigma_c^{(*)}$. *Phys. Rev.*, D96(1):014018, 2017.
44. Rui Chen, Zhi-Feng Sun, Xiang Liu, and Shi-Lin Zhu. Strong LHCb evidence supporting the existence of the hidden-charm molecular pentaquarks. 2019.
45. Lu Meng, Bo Wang, Guang-Juan Wang, and Shi-Lin Zhu. The hidden charm pentaquark states and $\Sigma_c\bar{D}^{(*)}$ interaction in chiral perturbation theory. 2019.
46. Roel Aaij et al. Observation of the doubly charmed baryon Ξ_{cc}^{++}. *Phys. Rev. Lett.*, 119(11):112001, 2017.
47. S. S. Gershtein, V. V. Kiselev, A. K. Likhoded, and A. I. Onishchenko. Spectroscopy of doubly charmed baryons: Xi(cc)+ and Xi(cc)++. *Mod. Phys. Lett.*, A14:135–146, 1999.
48. Chiaki Itoh, Toshiyuki Minamikawa, Kimio Miura, and Tsunetoshi Watanabe. Doubly charmed baryon masses and quark wave functions in baryons. *Phys. Rev.*, D61:057502, 2000.
49. Jian-Rong Zhang and Ming-Qiu Huang. Doubly heavy baryons in QCD sum rules. *Phys. Rev.*, D78:094007, 2008.
50. Zhi-Gang Wang. Analysis of the $\frac{1}{2}^+$ doubly heavy baryon states with QCD sum rules. *Eur. Phys. J.*, A45:267–274, 2010.
51. Zhi-Feng Sun and M. J. Vicente Vacas. Masses of doubly charmed baryons in the extended on-mass-shell renormalization scheme. *Phys. Rev.*, D93(9):094002, 2016.
52. Zalak Shah, Kaushal Thakkar, and Ajay Kumar Rai. Excited State Mass spectra of doubly heavy baryons Ω_{cc}, Ω_{bb} and Ω_{bc}. *Eur. Phys. J.*, C76(10):530, 2016.
53. Zalak Shah and Ajay Kumar Rai. Excited state mass spectra of doubly heavy Ξ baryons. *Eur. Phys. J.*, C77(2):129, 2017.
54. Xin-Zhen Weng, Xiao-Lin Chen, and Wei-Zhen Deng. Masses of doubly heavy-quark baryons in an extended chromomagnetic model. *Phys. Rev.*, D97(5):054008, 2018.
55. Rui Chen, Atsushi Hosaka, and Xiang Liu. Prediction of triple-charm molecular pentaquarks. *Phys. Rev.*, D96(11):114030, 2017.
56. Rui Chen, Fu-Lai Wang, Atsushi Hosaka, and Xiang Liu. Exotic triple-charm deuteronlike hexaquarks. *Phys. Rev.*, D97(11):114011, 2018.
57. F. Froemel, B. Julia-Diaz, and D. O. Riska. Bound states of double flavor hyperons. *Nucl. Phys.*, A750:337–356, 2005.
58. D. Ebert, R. N. Faustov, V. O. Galkin, and A. P. Martynenko. Mass spectra of doubly heavy baryons in the relativistic quark model. *Phys. Rev.*, D66:014008, 2002.
59. R. Machleidt, K. Holinde, and C. Elster. The Bonn Meson Exchange Model for the Nucleon Nucleon Interaction. *Phys. Rept.*, 149:1–89, 1987.
60. D. O. Riska and G. E. Brown. Nucleon resonance transition couplings to vector mesons. *Nucl. Phys.*, A679:577–596, 2001.
61. R. Machleidt. The High precision, charge dependent Bonn nucleon-nucleon potential (CD-Bonn). *Phys. Rev.*, C63:024001, 2001.
62. Xu Cao, Bing-Song Zou, and Hu-Shan Xu. Phenomenological analysis of the double pion production in nucleon-nucleon collisions up to 2.2 GeV. *Phys. Rev.*, C81:065201, 2010.